

# A Practical Approach to Causal Inference over Time

Martina Cinquini<sup>\*1</sup>, Isacco Beretta<sup>\*1</sup>, Salvatore Ruggieri<sup>1</sup>, Isabel Valera<sup>2</sup>

<sup>1</sup>Department of Computer Science, University of Pisa, Pisa, Italy

<sup>2</sup>Department of Computer Science, Saarland University, Saarbrücken, Germany

{martina.cinquini, isacco.beretta}@phd.unipi.it, salvatore.ruggieri@unipi.it, ivalera@cs.uni-saarland.de

## Abstract

In this paper, we focus on estimating the causal effect of an intervention over time on a dynamical system. To that end, we formally define causal interventions and their effects over time on discrete-time stochastic processes (DSPs). Then, we show under which conditions the equilibrium states of a DSP, both before and after a causal intervention, can be captured by a structural causal model (SCM). With such an equivalence at hand, we provide an explicit mapping from vector autoregressive models (VARs), broadly applied in econometrics, to linear, but potentially cyclic and/or affected by unmeasured confounders, SCMs. The resulting *causal VAR framework* allows us to perform *causal inference over time* from observational time series data. Our experiments on synthetic and real-world datasets show that the proposed framework achieves strong performance in terms of observational forecasting while enabling accurate estimation of the causal effect of interventions on dynamical systems. We demonstrate, through a case study, the potential practical questions that can be addressed using the proposed causal VAR framework.

## 1 Introduction

Dynamical systems often exhibit complex behaviors that unfold over time, leading to delayed responses and feedback loops. Importantly, understanding the causal effect of interventions within such systems is crucial across disciplines such as climate (Runge et al. 2019) and social sciences (Wunsch et al. 2022), where different time scales play a central role. For instance, monetary policy adjustments may have immediate effects on consumer spending, but their impact on inflation, employment, and economic growth only becomes evident in the medium-/long-term. Similarly, the consequences of human actions on climate change may take decades to manifest, with the risk of endorsing public policies that underestimate their relevance. To address these issues, it is essential to estimate the causal effect of interventions, or generally, to perform *causal inference over time*.

From the perspective of causality, Structural Causal Models (SCMs) provide a formal framework to perform causal inference from cross-sectional data. However, adapting existing methods to capture temporal dynamics remains a challenge (Bongers et al. 2021). Alternatively, temporal models, such as autoregressive models, offer practical methods

for time-series analysis and forecasting (Lütkepohl 2005), but their formalization of causal effects is limited. First, they model interventions as *shocks* applied at a specific point in time, with effects that fade away after a certain period (Hyvärinen et al. 2010; Moneta et al. 2011). Second, they rely on Granger causality (Granger 1969) which is concerned with how well one variable can predict another rather than identifying causal relationships between them.

Our work combines the strengths of both frameworks, i.e., SCMs and autoregressive models, to enable robust reasoning about the causal effect of interventions on dynamical systems over time. To that end, we first introduce a formal definition of causal interventions on discrete-time stochastic processes (DSPs), proposing two alternatives, additive and forcing interventions. Second, we establish conditions under which the equilibrium state of a DSP can be represented by an SCM. Third, we develop a framework that maps VARs to linear SCMs, handling potentially cyclic structures and unmeasured confounders. Finally, our practical framework for causal inference over time from observational time-series data is empirically validated on synthetic and real-world datasets.

**Related work** The works most closely related to ours are these from Mooij, Janzing, and Schölkopf (2013) and Bongers, Blom, and Mooij (2018), as they theoretically connect dynamical systems to the causal semantics of SCMs via the equilibration of deterministic and random differential equations, and thus are capable of modeling cyclic causal mechanisms (Bongers et al. 2021). Our approach differs from this line of work in two key aspects: i) we focus on *discrete-time* dynamical systems parameterized using *stochastic equations* which, as stated by Bongers, Blom, and Mooij (2018), become particularly challenging for continuous-time processes; and ii) our mapping from autoregressive DSPs to SCMs provides not only a theoretical but also, to the best of our knowledge, *the first data-driven framework for performing causal inference over time in dynamical systems*.

## 2 Preliminaries and background

### 2.1 Structural Causal Models

**Equation** A SCM  $\mathcal{M} = (\mathbf{F}, \mathbf{E})$  determines how a set of  $d$  endogenous (observed) random variables  $\mathbf{X} :=$

<sup>\*</sup>These authors contributed equally.

$\{X^{(1)}, \dots, X^{(d)}\}$  are obtained from a set of exogenous variables  $\mathbf{E} := \{E_1, \dots, E_d\}$ , with prior distribution  $p(\mathbf{E})$ , via a set of structural equations  $\mathbf{F} := \{X^{(i)} := f_i(\mathbf{PA}^{(i)}, \mathbf{E}^{(i)})\}_{i=1}^d$ . Each  $f_i$  computes  $X^{(i)}$  from its causal parents<sup>1</sup>  $\mathbf{PA}^{(i)} \subseteq \mathbf{X}$  and a set  $\mathbf{E}^{(i)} \subseteq \mathbf{E}$ . We refer to  $\mathbf{X}$  as a solution of  $\mathcal{M}$ . We assume  $\mathbf{PA}^{(i)}$  to be minimal, i.e., it only contains variables  $X^{(j)}$  such that  $\partial_{X^{(j)}} f_i \neq 0$ . This formulation extends the definition in (Pearl 2009) to include cycles as in (Bongers, Blom, and Mooij 2018).

**Graph** A SCM  $\mathcal{M}$  induces a directed graph  $\mathcal{G}_{\mathcal{M}} = (\mathcal{V}, \mathcal{E})$  that describes the functional dependencies in  $\mathbf{F}$ :  $\mathcal{V}$  is the set of nodes for which  $V_i$  represents  $X^{(i)}$  and  $\mathcal{E}$  is the set of the edges  $(V_i, V_j) \in \mathcal{E} \iff X^{(i)} \in \mathbf{PA}^{(j)}$ .

**Intervention** Besides describing the observational distribution  $p(\mathbf{X})$ , SCMs allow answering *interventional queries* about the effect of external manipulations, and enable *counterfactual queries* assessing what would have happened to a particular observation if one observed variable  $X^{(i)}$  had taken a different value. An intervention  $\mathcal{I}$  on a SCM  $\mathcal{M}$  yields a new SCM  $\mathcal{M}^{\mathcal{I}}$  for which one or more mechanisms  $f_i(\mathbf{PA}^{(i)}, \mathbf{E}^{(i)})$  change to  $\tilde{f}_i(\tilde{\mathbf{PA}}^{(i)}, \tilde{\mathbf{E}}^{(i)})$ , where  $\tilde{\mathbf{PA}}^{(i)} \subseteq \mathbf{PA}^{(i)}$  and  $\tilde{\mathbf{E}}^{(i)} \subseteq \mathbf{E}^{(i)}$ . We refer to a *hard intervention* when  $f_i$  is replaced by a constant value  $\alpha^{(i)}$ , and  $\tilde{\mathbf{PA}}^{(i)} = \tilde{\mathbf{E}}^{(i)} = \emptyset$ . This type of intervention is denoted by the do-operator  $do(X^{(i)} = \alpha^{(i)})$ . On the other hand, we refer to a *soft intervention* when at least one argument of  $f_i$  is retained. The causal effect CE of an intervention is evaluated in terms of differences between the values of the observable variables before and after the intervention  $\mathcal{I}$ , i.e.,

$$\text{CE}^{\mathcal{I}} = \mathbb{E}[\mathbf{X}^{\mathcal{I}} - \mathbf{X}]. \quad (1)$$

## 2.2 Discrete-time Stochastic Processes

A discrete-time (vector) stochastic process (DSP) is a function  $\mathbf{X} : T \times \Omega \rightarrow \mathbb{R}^d$  where  $t \in T$  is a time index in  $\mathbb{Z}$ , such that  $\mathbf{X}_t$  (which denotes  $\mathbf{X}(t, \cdot)$ ) is a random variable on a probability space  $(\Omega, \mathcal{F}, \mathbb{P})$ . We refer to  $\mathbf{X}(\omega)$  (which denotes  $\mathbf{X}(\cdot, \omega)$ ) as a *realization* or *trajectory* of  $\mathbf{X}$  and denote the  $i$ -th component of  $\mathbf{X}$  with  $X^{(i)}$ . Every DSP can be described through a difference equation (DE), i.e., a recurrence relation that allows computing  $\mathbf{X}_t$  based on its past values. DEs can be categorized into three types (Bongers, Blom, and Mooij 2018): ordinary difference equations (ODE) describing deterministic processes; random difference equations (RDE), which involve randomness in the initial state  $\mathbf{X}_0$  and in the evolution parameters (see App. A); and stochastic difference equations, which describe inherently stochastic trajectories.

**Equation** A stochastic difference equation (SDE) describes a DSP via a functional relationship of the form

$$\mathbf{X}_t = \mathbf{f}(\mathbf{X}_{<t}) + \mathbf{g}(\mathbf{X}_{<t}) \odot \boldsymbol{\varepsilon}_t, \quad (2)$$

<sup>1</sup>Unlike in acyclic SCMs,  $\mathbf{PA}^{(i)}$  loses its hierarchical interpretation since two nodes can be mutually parents.

where  $\mathbf{X}_{<t} := \{\mathbf{X}_{t-1}, \mathbf{X}_{t-2}, \dots\}$  represents the trajectory up to time  $t$ ,  $\mathbf{f}$  represents the system's deterministic mechanism, and the Hadamard product  $\mathbf{g} \odot \boldsymbol{\varepsilon}_t$  is the inhomogeneous stochastic part, where  $\boldsymbol{\varepsilon}_t$  denotes *white noise*, i.e.,  $\forall t, t' \in T \quad \mathbb{E}[\boldsymbol{\varepsilon}_t] = \mathbf{0}, \mathbb{E}[\boldsymbol{\varepsilon}_t^2] = \Sigma_{\boldsymbol{\varepsilon}}^2, \mathbb{E}[\boldsymbol{\varepsilon}_t \boldsymbol{\varepsilon}_{t'}] = \mathbf{0}$ . While for ODEs and RDEs trajectories  $\mathbf{X}(\omega)$  may asymptotically converge to an equilibrium, SDEs cannot exhibit such convergence due to the ongoing influence of  $\mathbf{g} \odot \boldsymbol{\varepsilon}_t$ .

**Graph** Analogously to SCMs, we can associate a directed graph  $\mathcal{G}_{\mathcal{D}}$  to a DE  $\mathcal{D}$ , consisting of nodes  $V_i$  representing individual components  $X^{(i)}$ , while an edge  $(V_i, V_j)$  is present if  $\exists k > 0$  such that  $\partial_{X^{(i)}} X_{t+k}^{(j)} \neq 0$  in  $\mathcal{D}$ .<sup>2</sup>

## 2.3 Vector Autoregressive models

In this paper, we focus on a specific type of SDE, the VAR model (Kilian and Lütkepohl 2017).

**Equation** Consider a  $d$ -dimensional vector-valued stationary time series  $\{\mathbf{X}_0, \dots, \mathbf{X}_T\}$  generated by a VAR model with lag  $p$ , where a lag represents the number of previous time steps used to predict the current value of each variable. Specifically, the VAR( $p$ ) model is defined by

$$\mathbf{X}_t = \boldsymbol{\nu} + \mathbf{A}_1 \mathbf{X}_{t-1} + \dots + \mathbf{A}_p \mathbf{X}_{t-p} + \mathbf{u}_t, \quad (3)$$

where  $\boldsymbol{\nu}$  is a  $d$ -dimensional vector of intercept terms,  $\{\mathbf{A}_i\}_{i=1}^p$  are  $(d \times d)$  matrices and  $\mathbf{u}_t$  is a  $d$ -dimensional white noise term. If the process  $\mathbf{X}_t$  is stable and stationary (Hamilton 1994), Equation 3 can also be written as

$$\begin{aligned} \mathbf{A}(L) \mathbf{X}_t &= \boldsymbol{\nu} + \mathbf{u}_t, \\ \text{with } \mathbf{A}(L) &:= \mathbf{I}_d - \mathbf{A}_1 L - \dots - \mathbf{A}_p L^p, \end{aligned} \quad (4)$$

where  $L$  is the *lag operator* such that  $L \mathbf{X}_t \equiv \mathbf{X}_{t-1}$  and  $\mathbf{I}_d$  is a  $d$ -dimensional identity matrix.

A key limitation of VARs is the inability to interpret the system in causal terms since the components of  $\mathbf{u}_t$  are cross-correlated and act as hidden confounders. A common approach to overcome this problem is to orthogonalize the noise terms. In this context, the process of *causal discovery*, i.e., inferring the causal structure of the data, is analogous to the one of SCMs (Hyvärinen et al. 2010; Moneta et al. 2013; Geiger et al. 2015; Malinsky and Spirtes 2018), and involves identifying a triangular matrix  $\hat{\mathbf{A}}_0$  such that  $\boldsymbol{\varepsilon}_t = \hat{\mathbf{A}}_0 \mathbf{u}_t$  consists of mutually uncorrelated elements. The transformed VAR, commonly known as the Structural VAR (SVAR) model in the literature (Kilian and Lütkepohl 2017), is defined by  $\hat{\mathbf{A}}_0 \mathbf{X}_t = \hat{\mathbf{A}}_0 \boldsymbol{\nu} + \hat{\mathbf{A}}_1 \mathbf{X}_{t-1} + \dots + \hat{\mathbf{A}}_p \mathbf{X}_{t-p} + \boldsymbol{\varepsilon}_t$ , where  $\hat{\mathbf{A}}_i = \hat{\mathbf{A}}_0 \mathbf{A}_i$ . From a modeling perspective, VAR and SVAR are equivalent, as any SVAR can be expressed in its reduced-form VAR by computing  $\mathbf{A}_i = \hat{\mathbf{A}}_0^{-1} \hat{\mathbf{A}}_i$  for  $i = 0, \dots, p$  in Eq. 3. Notably, choosing one over the other does not affect its causal interpretation, provided that  $\hat{\mathbf{A}}_0$  is known. For simplicity, in this work, we adopt the VAR notation, to introduce a *novel framework for causal inference over time, which complements the SVAR's causal discovery approach*.

<sup>2</sup>Depending on the type of DE, the derivative must be evaluated with respect to  $f_i$  or with respect to both  $f_i$  and  $g_i$  (see Equation 2).

**Graph** An edge  $(V_i, V_j)$  is present iff  $\exists k. \mathbf{A}_k[i, j] \neq 0$ .

### 3 Causal perspective on Discrete-time Stochastic Processes

This section provides the theoretical basis for causal inference over time. First, we formally define causal interventions on SDEs (§3.1). Then, we show how a SCM can be considered a compressed description of the asymptotic behavior of an underlying dynamical system (§3.2).

#### 3.1 Causal Interventions on SDEs

We define an intervention  $\mathcal{I}$  on a SDE  $\mathcal{D}$  as a modification of one or more component equations denoted by the mapping:

$$\mathcal{I} : f_i(\mathbf{PA}_{<t}^{(i)}) + g_i(\mathbf{PA}_{<t}^{(i)}) \odot \varepsilon_t \longmapsto \tilde{f}_i(\tilde{\mathbf{PA}}_{<t}^{(i)}) + \tilde{g}_i(\tilde{\mathbf{PA}}_{<t}^{(i)}) \odot \varepsilon_t, \forall t \geq t_{\mathcal{I}} \quad (5)$$

where  $\tilde{\mathbf{PA}}_{<t}^{(i)} \subseteq \mathbf{PA}_{<t}^{(i)}$ . Unlike SCMs, the intervention applies *starting from a specific time*  $t_{\mathcal{I}}$ . In other words, the process follows the original equations for  $t < t_{\mathcal{I}}$  and the modified ones for  $t \geq t_{\mathcal{I}}$ . We denote the modified SDE as  $\mathcal{D}^{\mathcal{I}}$  to generalize Eq. 1 to account for time. To differentiate between interventions on a SCM  $\mathcal{M}$  and on a SDE  $\mathcal{D}$ ,  $\mathcal{I}_{\mathcal{M}}$  and  $\mathcal{I}_{\mathcal{D}}$  will be respectively adopted when necessary.

**Definition 1** (Causal Effect over time (CE<sub>t</sub>)). Let  $\mathbf{X}$  be a solution of a specific SDE  $\mathcal{D}$ . We define the causal effect at time  $t$  of an intervention  $\mathcal{I}$  as

$$\text{CE}_t^{\mathcal{I}} := \mathbb{E}[\mathbf{X}_t^{\mathcal{I}} - \mathbf{X}_t | \mathbf{X}_{<t_{\mathcal{I}}}], \quad (6)$$

where  $\mathbf{X}^{\mathcal{I}}$  is the solution of the modified SDE  $\mathcal{D}^{\mathcal{I}}$ .

The interpretation of  $\text{CE}_t^{\mathcal{I}}$  is closely related to the causal effect of an intervention on a SCM (Eq. 1),  $\text{CE}_t^{\mathcal{I}}$ : while the latter measures the causal effect of an exogenous intervention,  $\text{CE}_t$  does so for any time step  $t$  of the DSP, i.e., *it measures the causal effect of an intervention over time*. Importantly, as we will show in the next section,  $\text{CE}_t^{\mathcal{I}} \rightarrow \text{CE}^{\mathcal{I}}$  as  $t \rightarrow \infty$ , i.e., there is an asymptotic correspondence between the two quantities.

#### 3.2 Mapping SDEs to SCMs

Given an SDE  $\mathcal{D}$  and its solution  $\mathbf{X}$ , we study the conditions on  $\mathcal{D}$  such that: i)  $\mathbf{X}_t$  converges in distribution to  $\mathbf{X}_{\infty}$  as  $t \rightarrow \infty$ ; and ii) there exists an SCM  $\mathcal{M}$  such that  $\mathbf{X}_{\infty}$  is a solution of  $\mathcal{M}$  and, for every intervention  $\mathcal{I}$ , it holds that  $(\mathbf{X}_{\infty})^{\mathcal{I}_{\mathcal{M}}} = (\mathbf{X}^{\mathcal{I}_{\mathcal{D}}})_{\infty}$ . While i) is automatically satisfied by any finite memory stationary process, ii) requires more careful analysis, as discussed below.

**A negative result from (Janzing, Rubenstein, and Schölkopf 2018)** Consider the stable bivariate system defined by the equations  $X_t = \varepsilon_t^x, Y_t = 0.5 \cdot X_{t-1} + \varepsilon_t^y$ . For every  $t$ ,  $X_t$  and  $Y_t$  are independent of each other. Consequently, the joint distribution  $p(X_t, Y_t)$  cannot capture the causal dependencies of the system ( $X$  causes  $Y$ ). The lack of causal information in the cross-sectional dimension arises because the variables are *localized in time*; their values change rapidly, leading to minimal or no correlation with

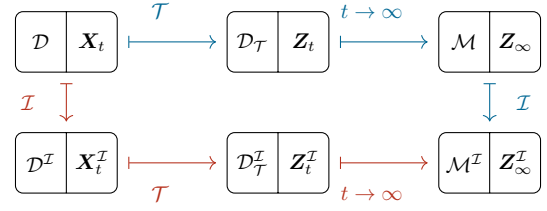


Figure 1:  $\mathcal{T}$ -transformation transfers causal information from the temporal to the cross-sectional dimension, and thus to the joint distribution  $P(\mathbf{Z}_t)$ . The diagram commutes, i.e., red and blue paths produce the same result.

their past values. On this specific point Janzing, Rubenstein, and Schölkopf (2018) provide an explicit negative result: without first making the variables de-localized in time, there is no SCM that can capture the SDE. In fact, our definition of intervention (Eq. 5) *acts on a variable of the system for a prolonged and indefinite period*.

**$\mathcal{T}$ -transformation** To overcome this limitation, (Janzing, Rubenstein, and Schölkopf 2018) propose a transformation of  $\mathbf{X}_t$  based on a frequency analysis of the time series.<sup>3</sup> Instead, our choice is inspired by the long-run normalized mean via the transformation  $\mathcal{T} : \text{DSP} \mapsto \text{DSP}$  defined by

$$\mathcal{T}(\mathbf{X})_t := \mathbf{Z}_t = \boldsymbol{\mu} + \frac{1}{\sqrt{t}} \sum_{i=1}^t (\mathbf{X}_i - \boldsymbol{\mu}), \quad (7)$$

where  $\boldsymbol{\mu} := \mathbb{E}[\mathbf{X}]$ .<sup>4</sup> Moreover,  $\mathbb{E}[\mathbf{Z}_{\infty}] = \mathbb{E}[\mathbf{X}_{\infty}] = \boldsymbol{\mu}$  so that for every intervention  $\mathcal{I}$ ,  $\text{CE}_{\infty}^{\mathcal{I}}$  (Eq. 6) *yields the same values*. However, unlike  $\mathbf{X}$ ,  $\mathbf{Z}$  can be mapped into an SCM that precisely models *its distribution shift over any intervention*, thereby satisfying property ii), represented as the commutativity of the diagram in Fig. 1.

It is important to clarify that  $\mathbf{Z}_t$  is not the process of interest, and the focus of the causal analysis remains on  $\mathbf{X}_t$ . However, due to the equivalence of long-run causal effects calculated in both processes, and the ability to associate  $\mathbf{Z}_t$  with the SCM that models these effects,  $\mathbf{Z}_t$  serves as a convenient intermediate mathematical tool. To demonstrate how this transformation ensures these desirable properties, we will focus on the subclass of linear systems, particularly on VAR models. The reason for this choice is twofold. First, linear models, despite their simplicity, are still on par performance-wise with state-of-the-art Machine-Learning based forecast techniques (Toner and Darlow 2024), in particular when dealing with stochastic time series (Parmezan, Souza, and Batista 2019). Second, the mathematical treatment of interventions and the estimation of causal effects is particularly straightforward to implement and interpret, making this a useful first step for a possible extension to the nonlinear case.

<sup>3</sup>Our  $\mathbf{Z}_t$  (Eq. 7) can also be interpreted as a form of discrete Fourier transform of the time-series  $\mathbf{X}_{1:t}$  with frequency zero.

<sup>4</sup>The expectation here is taken over time as well. Nonetheless, for stationary processes, this simplifies to  $\mathbb{E}[\mathbf{X}] = \mathbb{E}[\mathbf{X}_t]$  for all  $t$ .

## 4 From Vector Autoregressive models to Structural Causal Models

In this section, we show that linear SCMs can model the long-term effects of stable VARs, explaining the properties of its DSP equilibrium (§4.1). Then, we provide implementations of two types of causal interventions, leveraging the strengths of the VAR framework (§4.2). Finally, we discuss the practical implications of our theoretical results (§4.3).

### 4.1 Mapping from VARs to SCMs

We provide the explicit mapping from VARs to linear SCMs in the following theorem (proved in App. B.2).

**Theorem 1.** Given a stable VAR( $p$ )  $\mathcal{D}$  defined by Eq. 3, there exists a linear SCM  $\mathcal{M}$  with structural equations<sup>5</sup>

$$\tilde{\mathbf{X}} = \tilde{\mathbf{A}}\tilde{\mathbf{X}} + \tilde{\mathbf{u}}, \quad (8)$$

where  $\tilde{\mathbf{A}} := [\mathbf{A}_1 + \dots + \mathbf{A}_p]$  and  $\tilde{\mathbf{u}} \sim \mathcal{N}(\mathbf{0}, \Sigma_{\tilde{\mathbf{u}}})$ ,

such that, given the transformation  $\mathbf{Z}_t = \frac{1}{\sqrt{t}} \sum_{i=1}^t \mathbf{X}_i$ , the following properties hold:

1.  $\mathcal{D}$  and  $\mathcal{M}$  share the same *causal graph*, i.e.,  $\mathcal{G}_{\mathcal{M}} = \mathcal{G}_{\mathcal{D}}$ ;
2. The *observational distribution* induced by  $\mathcal{D}$  at equilibrium  $p(\mathbf{Z}_{\infty})$  is equal to the one induced by  $\mathcal{M}$ ,  $p(\tilde{\mathbf{X}})$ ;
3. The *interventional distribution*  $p(\mathbf{Z}_{\infty}^{\mathcal{I}})$  is equal to the one induced by the same intervention on  $\mathcal{M}$ ,  $p(\tilde{\mathbf{X}}^{\mathcal{I}_{\mathcal{M}}})$ .

**Remark.** Note that due to the influence of time in VARs, the equivalent SCMs at equilibrium, while linear, may lead to cycles in the causal graph (see, e.g., Fig. 2c) and correlations between the exogenous variables, captured by the full covariance matrix  $\Sigma_{\tilde{\mathbf{u}}}$  in Eq. 8. Note also that the above Theorem implies that there is a direct relationship between interventions on DSPs,  $\mathcal{I}$ , and interventions on SCMs, here denoted by  $\mathcal{I}_{\mathcal{M}}$ . Refer to App. B.2 for further details.

### 4.2 Implementation of Causal Interventions

Different application scenarios may need different types of interventions. Consider a government’s fiscal policy. In such a setting, a feasible approach would be to implement an *additive intervention* in the form of an annual tax increase of, e.g., 300 euros per household on top of existing taxes. Alternatively, in other scenarios, e.g., when studying the effect of the *key European Central Bank’s interest rate* (Belke and Polleit 2007), a more natural choice is to implement a *forcing intervention* that enforces the convergence of an observed variable (e.g., interest rate) to a target value. In the following, we propose an implementation for VARs of these two forms of interventions, showing their effects on the system and discussing their stability conditions.

**Additive Interventions** Given a stable VAR( $p$ ) as in Eq. 4, we define an additive intervention  $\mathcal{I}_a$  at time  $t_{\mathcal{I}}$  with force  $\mathbf{F}$  as the mapping:

$$\begin{aligned} \mathcal{I}_a : \mathbf{A}(L)\mathbf{X}_t = \boldsymbol{\nu} + \mathbf{u}_t &\longmapsto \\ \mathbf{A}(L)\mathbf{X}_t = \boldsymbol{\nu} + \mathbf{u}_t + \mathbb{I}(t \geq t_{\mathcal{I}})\mathbf{F}, &\quad (9) \end{aligned}$$

<sup>5</sup>For simplicity we set  $\boldsymbol{\nu} = \mathbf{0}$ , i.e., we assume  $\mathbb{E}[\mathbf{X}_t] = \mathbf{0}$ . The theorem applies in the general case up to a translation of both the VAR and the associated SCM.

where  $\mathbb{I}(t \geq t_{\mathcal{I}})$  is the indicator function, which equals 1 if  $t \geq t_{\mathcal{I}}$ , otherwise 0. In other words, we perform a translation while keeping the process dynamics unchanged. In such case, the temporal causal effect  $\text{CE}_t$  is deterministic and takes values  $\text{CE}_t = 0$  for  $t < t_{\mathcal{I}}$  while, for  $k \geq 0$ :

$$\text{CE}_{t_{\mathcal{I}}+k} = \sum_{l=0}^k \Phi_l \mathbf{F},$$

where  $\Phi$  is the *impulse response function* of the VAR model. Refer to App. B.1 for further details.

**Remark.** For this type of intervention,  $\text{CE}_t$  is deterministic and does not depend on the specific trajectory. The same property can be observed on the linear SCM associated with the process, defining the intervention in a similar way:  $\tilde{\mathbf{X}} = \tilde{\mathbf{A}}\tilde{\mathbf{X}} + \tilde{\mathbf{u}}$  changes into  $\tilde{\mathbf{X}} = \tilde{\mathbf{A}}\tilde{\mathbf{X}} + \mathbf{F} + \tilde{\mathbf{u}}$ .

**Stability** Additive intervention preserves the stability regardless of the value of  $\mathbf{F}$ , since  $\mathbf{A}(L)$  does not change. See App. B.1 for stability conditions of VARs.

**Forcing Interventions** We define a forcing intervention  $\mathcal{I}_f$  at time  $t_{\mathcal{I}}$  with force  $\mathbf{F}$  and target value  $\hat{\mathbf{X}}$  as:

$$\begin{aligned} \mathcal{I}_f : \mathbf{A}(L)\mathbf{X}_t = \boldsymbol{\nu} + \mathbf{u}_t &\longmapsto \\ \mathbf{A}(L)\mathbf{X}_t = \boldsymbol{\nu} + \mathbf{u}_t + \mathbb{I}(t \geq t_{\mathcal{I}})\mathbf{F} \odot (\hat{\mathbf{X}} - \mathbf{X}_t). &\quad (10) \end{aligned}$$

We assume  $\mathbf{F}$  to be positive in each component. This intervention acts as an attraction towards  $\hat{\mathbf{X}}$ , and  $\mathbf{F}$  modulates the intensity of the attraction force. Applying an intervention on a single component  $X^{(i)}$  toward the fixed value  $\hat{X}$  and letting  $F^{(i)} \rightarrow +\infty$  yields the do operator  $do(X^{(i)} = \hat{X})$ . We refer to (Mooij, Janzing, and Schölkopf 2013) for a detailed discussion of this point.

**Stability** Forcing interventions  $\mathcal{I}_f$  perturb the system dynamics by modifying the operator  $\mathbf{A}(L)$ . Specifically, by shifting the term  $\mathbf{F} \odot \mathbf{X}_t$  to the left of the equation and rewriting it in matrix form as  $\mathbf{F}_{diag}\mathbf{X}_t$ , we obtain  $\tilde{\mathbf{A}}(L) := \mathbf{A}(L) + \mathbf{F}_{diag}$ . Hence, the stability of the intervened system is not guaranteed (we provide an example in App. B.3), and it is necessary to verify that *all the eigenvalues of  $\tilde{\mathbf{A}}(L)$  are still inside the unit circle*. Intuitively, the stability of an observational system often relies on negative feedback loops. Fixing one variable can disrupt this balance, leading to runaway behavior. For example, turning off a pressure release valve in a pressurized tank can cause the pressure to build up uncontrollably, eventually leading to an explosion.

### 4.3 Practical implications

**Causal queries** Our formulation of causal interventions on VARs differs from the standard approach based on Granger causality by being closer to that of SCMs. Consequently, it enables the generalization of interventional and counterfactual queries to account for time (see App. C). That is, it allows for answering the following causal questions:

- **Forecasted Interventions** What are the expected effects on an individual trajectory (or a population) when intervening in the present, and how do they vary over time?

- **Retrospective Counterfactuals** What would have happened to an individual trajectory if an intervention had been applied at a specific point in the past? What state would it be in now?

Both causal queries acquire a meaning embedded in the temporal dimension in terms of *forecasting for the future* (§5.2) and *retrospection for the past* (App. D.3), respectively.

**Expressiveness and universality** VARs, despite their linearity, possess a high level of expressiveness (Kilian and Lütkepohl 2017). In fact, the Wold decomposition Theorem (Wold 1938) implies that the dynamics of *any purely non-deterministic covariance-stationary process can be approximated arbitrarily well by an autoregressive model, making them universal approximators*. In practice, linear autoregressive models are broadly used in time-series analysis. Yet, we intend to explore non-linear DSPs in future work, as they may lead to better convergence rates and allow for causal interpretation of a broader family of dynamical models.

**Feedback loops** To properly understand complex systems, it is often useful to model feedback loops between their variables. Time-series models naturally capture this property, while SCMs require significant reformulation. The theory of cyclic SCMs has seen a significant advancement in recent years (Bongers et al. 2021), but practical approaches, both for causal discovery and causal inference, are still underdeveloped (Bongers et al. 2016; Lorbeer and Mohsen 2023). Our formalization of causal inference on VARs is a step forward in this direction.

**Fitting** VARs estimation is typically performed using ordinary least squares. Various alternative methods are available, both in terms of constrained optimization (e.g., to use prior knowledge about some coefficients of the VAR matrices (Sims 1980)) and within a Bayesian framework (Koop, Korobilis et al. 2010). Refer to (Lütkepohl 2005, chapters 3,4,5) for a comprehensive discussion. Importantly, although VARs are most commonly used on time-series data (i.e., data from one single unit across a period of time), there are approaches tailored to the analysis of *panel data* (i.e., the evolution of many units over time) (Sigmund and Ferstl 2021); and *cross-sectional data* (i.e., many individuals at a single point of time), provided that they have at least some proxy variables of time (Deaton 1985). Such approaches open up a promising line of future work that can further generalize VARs applicability for causal reasoning over time.

## 5 Empirical evaluation

In this section, we evaluate VAR models’ accuracy and expressiveness in multivariate time series, focusing on two forecasting dimensions: observational (§5.1) and interventional (§5.2). Additional results and in-depth descriptions can be found in App. D.

**Datasets** We rely on two synthetic datasets, German<sup>6</sup> and Pendulum, and the real-world Census dataset<sup>7</sup>. German sim-

<sup>6</sup>This dataset is inspired on <https://archive.ics.uci.edu/dataset/144/statlog+german+credit+data>

<sup>7</sup><https://data.census.gov/>

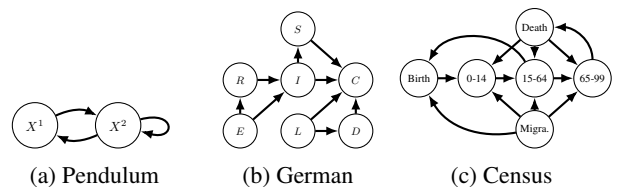


Figure 2: **Causal graphs**. The causal graph for (a) and (b) is known, while for (c), it is assumed. In (b), nodes are labeled with the initials of each feature: Expertise, Responsibility, Loan Amount, Duration, Income, Savings, and Credit Score. In (c), 0 – 14, 15 – 64, and 65 – 99 represent age groups.

ulates a loan approval scenario with seven variables. Pendulum is a two-variable system where  $X^{(1)}$  operates as a stabilizer for  $X^{(2)}$ , which exhibits a divergent dynamic. Census includes demographic variables across three age groups, along with migration, birth, and death rates from 1992 to 2023 for 50 countries. Fig. 2 illustrates the causal graphs for all datasets. See App. D for further details.

**Metrics** We measure the discrepancy between the  $h$ -steps forecast  $\hat{X}_{t+h} | X_{<t}$  and the true value  $X_{t+h}$  on the test set  $X_{test}$ . We report Mean Absolute Error (MAE) focusing on the target variables (i.e., *Credit Score* for German,  $X^{(1)}$  for Pendulum, and age groups for Census). See App. D.1 for other metrics. All results are averaged over ten runs.

### 5.1 Observational Forecasting

**Baselines** We compare VAR with three relevant works: i) DLinear (Zeng et al. 2023), a decomposition-based linear model that separates trend and seasonal components; ii) TSMixer (Chen et al. 2023), a Multi-layer Perceptron (MLP) based model that focuses on mixing time and feature dimensions; iii) TiDE (Das et al. 2023), a MLP based encoder-decoder model. To assess the effectiveness of the forecasting methods, we introduce an observational oracle forecaster that has full knowledge about the true data generating process and produces the optimal predictor, i.e.,  $\hat{X}_{t+h} | X_{<t} = \mathbb{E}[X_{t+h} | X_{<t}]$ .

**How does the VAR performance compare with SOTA models for forecasting multivariate time series?** The observational forecasting results in Table 1 show performance across varying data sizes (i.e., number of instances) and forecast horizons for all datasets. VAR emerges as the top-performing model, consistently matching or closely approaching Oracle’s scores for all datasets. DLinear usually achieves predictive accuracy close to VAR for 1-step forecasts, presumably due to the common linear nature of both models. TiDE and TSMixer consistently underperform compared to VAR and DLinear for German and Pendulum. For all models (including Oracle), performance on the Pendulum dataset is uniformly worse than on the German, highlighting the greater challenge in forecasting given the system’s stronger stochasticity and variables changing more rapidly over time. On Census, VAR and TiDE provide the best results, TiDE slightly outperforming VAR in 5-step horizon.

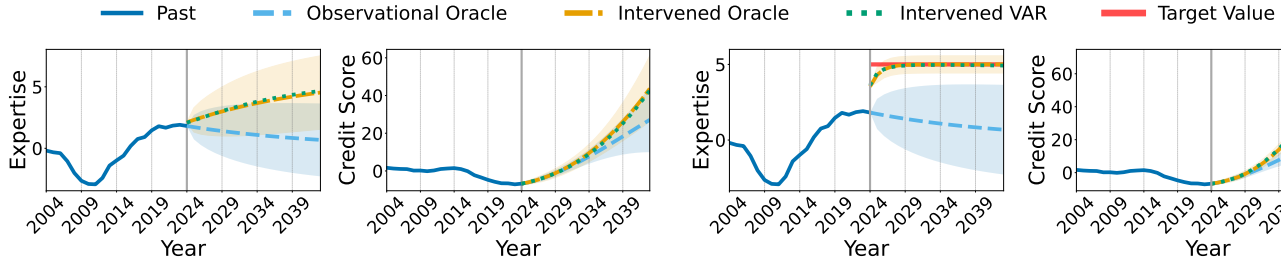


Figure 3: **Additive Intervention.** (Left) Intervention on *Expertise* with  $F = 0.2$ . (Right) Effect on *Credit Score*. Shaded regions in both plots denote 95% confidence bounds.

Table 1: **Observational Forecasting.** MAE scores (*lower is better*) for VAR, DLinear (Zeng et al. 2023), TiDE (Das et al. 2023) and TSMixer (Chen et al. 2023). Results averaged over 10 runs. Due to space limitations, standard deviations are reported in App. D.1. Best model in bold, Oracle in typewriter. For Census, size equals the number of countries times the number of years.

Dataset	Size	Horizon	Observational Forecasting				
			Oracle	VAR	DLinear	TiDE	TSMixer
German	100	1	.004	<b>.008</b>	.009	.011	.014
Pendulum		5	.042	<b>.043</b>	<b>.043</b>	.218	.217
German	100	10	.014	<b>.055</b>	<b>.055</b>	.094	.139
Pendulum		5	.399	<b>.420</b>	.440	1.43	1.43
German	500	1	.004	<b>.004</b>	<b>.004</b>	.011	.014
Pendulum		5	.042	<b>.042</b>	<b>.042</b>	.218	.217
German	500	10	.014	<b>.015</b>	<b>.015</b>	.093	.135
Pendulum		5	.399	<b>.401</b>	.405	1.43	1.43
Census	50 × 32	1	-	<b>.001</b>	.006	<b>.001</b>	.008
		5	-	.017	.025	<b>.014</b>	.024

## 5.2 Interventional Forecasting

We evaluate the causal VAR’s forecast in estimating the causal effects on German. See App. D.2 for other datasets.

**Baselines** Since state-of-the-art methods do not allow computing the causal effect of interventions on dynamical systems, we use an oracle forecaster as a benchmark for theoretically optimal performance. Specifically, the ground truth values are estimated as  $\text{CE}_{t+h} = \mathbb{E}[\mathbf{X}_{t+h}^I - \mathbf{X}_{t+h} | \mathbf{X}_{<t}]$ , while the predicted values from the proposed VAR framework as  $\hat{\text{CE}}_{t+h} = (\hat{\mathbf{X}}_t^I - \hat{\mathbf{X}}_{t+h}) | \mathbf{X}_{<t}$ .

**Interventions** We perform causal interventions on the root node *Expertise* and observe the effect on the target variable *Credit Score*. For the additive case, we apply  $F = 0.2$ , while for forcing, we use  $F = 1$  with a target value of  $\hat{E} = 5$ .

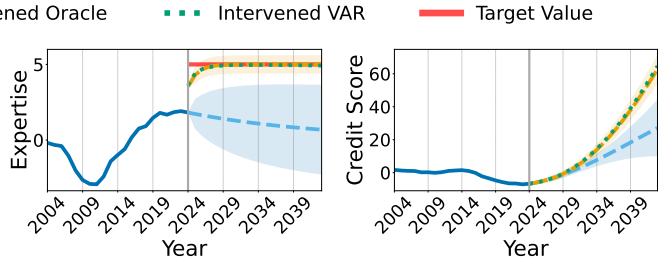


Figure 4: **Forcing Intervention.** (Left) Intervention on *Expertise* with  $F = 1$  and target  $\hat{E} = 5$ . (Right) Effect on *Credit Score*. Note that confidence bounds are narrower w.r.t. Fig. 3.

Table 2: **Interventional Forecasting.** MAE scores (*lower is better*) for the proposed causal VAR framework on the German dataset. Results averaged over 10 runs, with standard deviation in subscript. Scores are scaled by a factor of  $10^2$  to ease readability.

Dataset	Size	Horizon	Interventional Forecasting	
			Additive	Forcing
German	100	1	.000 <sub>.000</sub>	.000 <sub>.000</sub>
		10	.043 <sub>.028</sub>	.364 <sub>.297</sub>
	500	1	.000 <sub>.000</sub>	.000 <sub>.000</sub>
		10	.018 <sub>.014</sub>	.115 <sub>.081</sub>

These values are selected for illustrative purposes such that the long-term expected value of *Expertise* is the same for both interventions (i.e., 5). See App. D.2 for other variants.

**How do additive and forcing interventions affect the system dynamics?** Fig. 3 illustrates the additive intervention. *Expertise* is a variable that typically necessitates several years for acquisition in practical scenarios. The causal VAR accurately captures such delayed impact as its effect on *Credit Score* appears after several years. As the system maintains its dynamic characteristics unchanged, the forecasted covariance remains the same even after the intervention. Fig. 4 shows the forcing intervention, where the interventional forecasting exactly aligns with the target value. Moreover, we stress that even for a low value of  $F$ , the forcing intervention resembles a do-intervention (shrinking the variances significantly) even though theoretical convergence is guaranteed only for  $F \rightarrow \infty$ .

**How accurate is the causal VAR framework in estimating the causal effect of interventions over time?** Table 2 summarizes results on interventional forecasting, showing errors with varying data size and forecast horizons. At 1-step, both interventions lead to perfect performance since *Credit Score* is a slow-changing variable and requires at least 3 time steps for an intervention to take effect. At 10-step, our causal effect estimates remain highly accurate.

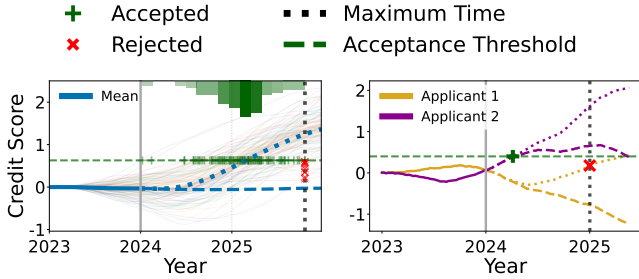


Figure 5: **German**. Effect of increasing *Expertise* on *Credit Score*. (Left) The time each loan applicant takes to cross or not the acceptance threshold. The histogram shows the distribution of crossing times. (Right) Comparison of two loan applicants, i.e., trajectories, with similar scores at intervention time. After the intervention, they diverge significantly, with only an applicant being accepted at the maximum time. Forecasts are dashed for observational and dotted for interventional.

## 6 Use cases

In this section, we show real-world scenarios where estimating causal effects over time represents a useful step toward a realistic modeling of the phenomena. We focus on the German and Census datasets, presenting two analyses for each. For German, Fig. 5 illustrates the effect of increasing *Expertise* by  $F = 0.38$  on *Credit Score*.

### German 1 – Same intervention, different outcomes.

The left panel of Fig. 5 shows the distribution of the time required for loan applicants to cross or not the acceptance threshold after the intervention. Access to this information allows quantification of intervention efficacy, identification of credit-building patterns, and infer the key factors influencing loan eligibility outcomes. It can also inform the recommendation of actions (e.g. in algorithmic recourse (Karimi et al. 2022)) within a reasonable timeframe, fostering trust in the system and promoting user acceptance.

**German 2 – Similar cross-sectional values, different causal effects over time.** The right panel of Fig. 5 shows trajectories that, while seeming similar at a given time, may have significantly divergent historical and future behaviors. For instance, the purple trajectory may have autonomously crossed the threshold without intervention, whereas in the case of the yellow one, the applied intervention may be inadequate to ensure the desired outcome. Such divergence highlights the importance of moving beyond models that rely only on cross-sectional data, motivating the need for techniques, such as the proposed causal VAR framework, that capture individual applicant behavior over time.

For Census, Fig. 6 presents two additive interventions across all countries.

**Census 1 – Impact of Births on Avg. Age.** The left panel of Fig. 6 shows the increase on *Births* with  $F = 0.004$  and its effect on the population’s average age (computed as a weighted mean of age groups). The force value means that *Births* increase by 0.4% of each country’s total population

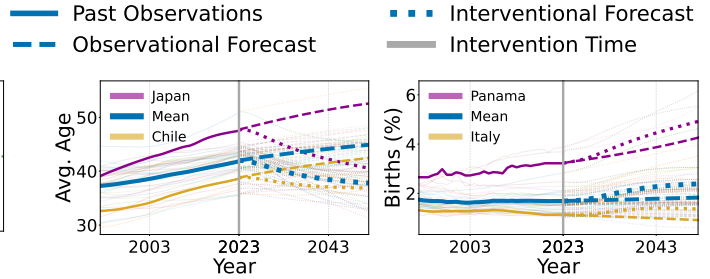


Figure 6: **Census**. Additive intervention across all countries. (Left) Intervention on *Births* with  $F = 0.004$  and its effect on the population’s average age. (Right) Intervention on *Migration* with  $F = 0.04$  and its effect on *Births*. In both plots, we highlight two countries (one above and one below the mean) to illustrate the differences after the intervention. Forecasts are dashed for observational and dotted for interventional.

every year. Examining how they affect population age over time could allow policymakers to identify which countries might benefit most from specific types of demographic interventions and evaluate the long-term viability of systems. We can also observe that the intervention in Japan causes a more evident decrease in the average age than in Chile.

**Census 2 – Impact of Migration on Births.** The right panel of Fig. 6 reports how a 4% growth in *Migration* w.r.t. the total population influences *Birth* rates. We observe that increased migration leads to a rise in births. However, its impact is less evident (observational and interventional forecasting trajectories are closer) compared to the result on the average age shown in Fig. 6 (left panel).

## 7 Concluding remarks

In this work, we have established a link between discrete-time dynamical systems at equilibrium and SCMs. Moreover, we have provided an explicit procedure for mapping VARs to linear SCMs and demonstrated that, under specific model stability conditions, interventions on the dynamical system and the SCM yield equivalent results. To conduct causal inference over time, we have introduced two classes of interventions (additive and forcing) for VARs.

**Limitations** When systems exhibit strongly nonlinear dynamics, linear VARs may prove less effective than alternative nonlinear approaches. Moreover, our framework requires prior knowledge of the causal graph. In scenarios where this information is lacking, the process of causal discovery can present significant challenges.

**Future work** We will investigate the use of non-linear DSPs, as they may lead to better convergence rates and allow for causal interpretation of a broader family of dynamical models. Moreover, our work opens several interesting research directions (§4.3 for concrete examples) and applications (e.g. causal inference over time in high-dimensional contexts such as climate science).

## References

- Anderson, T. 1994. *The Statistical Analysis of Time Series*. Wiley Series in Probability and Statistics.
- Arnold, L.; Jones, C. K.; Mischaikow, K.; Raugel, G.; and Arnold, L. 1995. *Random dynamical systems*. Springer.
- Bareinboim, E.; Correa, J. D.; Ibeling, D.; and Icard, T. 2022. On Pearl’s Hierarchy and the Foundations of Causal Inference. In *Probabilistic and Causal Inference*, volume 36 of *ACM Books*, 507–556. ACM.
- Belke, A.; and Polleit, T. 2007. How the ECB and the US Fed set interest rates. *Applied Economics*, 39(17): 2197–2209.
- Bhattacharya, R.; and Majumdar, M. 2003. Random dynamical systems: a review. *Economic Theory*, 23: 13–38.
- Bongers, S.; Blom, T.; and Mooij, J. M. 2018. Causal modeling of dynamical systems. *arXiv preprint arXiv:1803.08784*.
- Bongers, S.; Forré, P.; Peters, J.; and Mooij, J. M. 2021. Foundations of structural causal models with cycles and latent variables. *The Annals of Statistics*, 49(5): 2885–2915.
- Bongers, S.; Peters, J.; Schölkopf, B.; and Mooij, J. M. 2016. Structural Causal Models: Cycles, Marginalizations, Exogenous Reparametrizations and Reductions. *CoRR*, abs/1611.06221.
- Chen, S.; Li, C.; Arik, S. Ö.; Yoder, N. C.; and Pfister, T. 2023. TSMixer: An All-MLP Architecture for Time Series Forecasting. *Trans. Mach. Learn. Res.*, 2023.
- Das, A.; Kong, W.; Leach, A.; Mathur, S.; Sen, R.; and Yu, R. 2023. Long-term Forecasting with TiDE: Time-series Dense Encoder. *Trans. Mach. Learn. Res.*, 2023.
- Deaton, A. 1985. Panel data from time series of cross-sections. *Journal of econometrics*, 30(1-2): 109–126.
- Edwards, R. M.; Lee, K. Y.; and Ray, A. 1992. Robust optimal control of nuclear reactors and power plants. *Nuclear Technology*, 98(2): 137–148.
- Geiger, P.; Zhang, K.; Schoelkopf, B.; Gong, M.; and Janzing, D. 2015. Causal Inference by Identification of Vector Autoregressive Processes with Hidden Components. In Bach, F.; and Blei, D., eds., *Proceedings of the 32nd International Conference on Machine Learning*, volume 37 of *Proceedings of Machine Learning Research*, 1917–1925. Lille, France: PMLR.
- Granger, C. W. 1969. Investigating causal relations by econometric models and cross-spectral methods. *Econometrica: journal of the Econometric Society*, 424–438.
- Hamilton, J. D. 1994. *Time Series Analysis*.
- Herzen, J.; Lässig, F.; Piazzetta, S. G.; Neuer, T.; Tafti, L.; Raille, G.; Van Pottelbergh, T.; Pasiëka, M.; Skrodzki, A.; Huguenin, N.; et al. 2022. Darts: User-friendly modern machine learning for time series. *Journal of Machine Learning Research*, 23(124): 1–6.
- Hildebrand, F. B. 1987. *Introduction to numerical analysis*. Courier Corporation.
- Hyvärinen, A.; Zhang, K.; Shimizu, S.; and Hoyer, P. O. 2010. Estimation of a Structural Vector Autoregression Model Using Non-Gaussianity. *J. Mach. Learn. Res.*, 11: 1709–1731.
- Janzing, D.; Rubenstein, P.; and Schölkopf, B. 2018. Structural causal models for macro-variables in time-series. *arXiv preprint arXiv:1804.03911*.
- Jornet, M. 2023. Theory and methods for random differential equations: a survey. *SeMA Journal*, 80(4): 549–579.
- Karimi, A.-H.; Barthe, G.; Schölkopf, B.; and Valera, I. 2022. A survey of algorithmic recourse: contrastive explanations and consequential recommendations. *ACM Computing Surveys*, 55(5): 1–29.
- Kilian, L.; and Lütkepohl, H. 2017. *Structural vector autoregressive analysis*. Cambridge University Press.
- Kingma, D. P.; and Ba, J. 2015. Adam: A Method for Stochastic Optimization. In *ICLR (Poster)*.
- Koop, G.; Korobilis, D.; et al. 2010. Bayesian multivariate time series methods for empirical macroeconomics. *Foundations and Trends® in Econometrics*, 3(4): 267–358.
- Lasota, A.; and Mackey, M. C. 1989. Stochastic perturbation of dynamical systems: The weak convergence of measures. *Journal of Mathematical Analysis and Applications*, 138(1): 232–248.
- Lorbeer, B.; and Mohsen, M. 2023. Comparative Study of Causal Discovery Methods for Cyclic Models with Hidden Confounders. In *CogMI*, 103–111. IEEE.
- Łoskot, K.; and Rudnicki, R. 1995. Limit theorems for stochastically perturbed dynamical systems. *Journal of applied probability*, 32(2): 459–469.
- Lütkepohl, H. 2005. *New introduction to multiple time series analysis*. Springer Science & Business Media.
- Malinsky, D.; and Spirtes, P. 2018. Causal Structure Learning from Multivariate Time Series in Settings with Unmeasured Confounding. In *CD@KDD*, volume 92 of *Proceedings of Machine Learning Research*, 23–47. PMLR.
- Moneta, A.; Chlaß, N.; Entner, D.; and Hoyer, P. 2011. Causal search in structural vector autoregressive models. In *NIPS Mini-Symposium on Causality in Time Series*, 95–114. PMLR.
- Moneta, A.; Entner, D.; Hoyer, P. O.; and Coad, A. 2013. Causal inference by independent component analysis: Theory and applications. *Oxford Bulletin of Economics and Statistics*, 75(5): 705–730.
- Montgomery, D. C.; Jennings, C. L.; and Kulahci, M. 2015. *Introduction to time series analysis and forecasting*. John Wiley & Sons.
- Mooij, J. M.; Janzing, D.; and Schölkopf, B. 2013. From Ordinary Differential Equations to Structural Causal Models: the deterministic case. In Nicholson, A. E.; and Smyth, P., eds., *Proceedings of the Twenty-Ninth Conference on Uncertainty in Artificial Intelligence, UAI 2013, Bellevue, WA, USA, August 11-15, 2013*. AUAI Press.
- Parmezan, A. R. S.; Souza, V. M.; and Batista, G. E. 2019. Evaluation of statistical and machine learning models for time series prediction: Identifying the state-of-the-art and the best conditions for the use of each model. *Information sciences*, 484: 302–337.
- Pearl, J. 2009. *Causality*. Cambridge university press.

Runge, J.; Bathiany, S.; Bollt, E.; Camps-Valls, G.; Coumou, D.; Deyle, E.; Glymour, C.; Kretschmer, M.; Mahecha, M. D.; Muñoz-Marí, J.; et al. 2019. Inferring causation from time series in Earth system sciences. *Nature communications*, 10(1): 2553.

Sigmund, M.; and Ferstl, R. 2021. Panel vector autoregression in R with the package panelvar. *The Quarterly Review of Economics and Finance*, 80: 693–720.

Sims, C. A. 1980. Macroeconomics and reality. *Econometrica: journal of the Econometric Society*, 1–48.

Toner, W.; and Darlow, L. N. 2024. An Analysis of Linear Time Series Forecasting Models. In *Forty-first International Conference on Machine Learning*.

Wold, H. 1938. *A study in the analysis of stationary time series*. Ph.D. thesis, Almqvist & Wiksell.

Wunsch, G.; Russo, F.; Mouchart, M.; and Orsi, R. 2022. Time and causality in the social sciences. *Time & Society*, 31(2): 177–204.

Zeng, A.; Chen, M.; Zhang, L.; and Xu, Q. 2023. Are Transformers Effective for Time Series Forecasting? *Proceedings of the AAAI Conference on Artificial Intelligence*, 37(9): 11121–11128.

## A Difference Equations and Stochastic Processes Equilibration

Difference Equations can serve as discrete approximations of differential equations, sharing some fundamental theoretical properties. In many applications, the former are approximation tools to simulate the latter numerically. As with differential equations, it can be beneficial to introduce stochastic components into the equation to model phenomena that are not entirely predictable. This unpredictability may stem from incomplete knowledge of the relevant variables of the process or its intrinsic randomness. We will denote by DE the class of difference equations in general, regardless of whether they are deterministic or not. Including stochastic components in differential equations gives rise to various classes of equations. This section introduces the notions of Ordinary and Random Difference Equations. Understanding these concepts is helpful for contextualizing our work, and for clarifying how it extends the ideas presented in (Mooij, Janzing, and Schölkopf 2013).

### A.1 Difference equations

**Ordinary Difference Equation** An Ordinary Difference Equation (ODE) is an expression that describes the evolution of an indexed variable  $x_t$  through a functional relationship

$$x_t = f(x_{<t}),$$

where  $x_{<t} := \{x_{t-1}, x_{t-2}, \dots\}$  represents the past of  $x_t$ . Specifically, a  $p^{\text{th}}$ -order ODE is an expression where the preceding variables of  $x_t$  include up to  $x_{t-p}$ , i.e.,  $x_{<t} = \{x_{t-i}\}_{i=1}^p$ .

**Random Difference Equation** A Random Difference Equation (RDE) is a DE of the form

$$\mathbf{X}_t = f(\mathbf{X}_{<t}, \varepsilon), \quad (11)$$

where  $\varepsilon : \Omega \rightarrow \mathbb{R}^e$  is a random variable<sup>8</sup> and such that for every  $\omega \in \Omega$ , the equation

$$\mathbf{X}_t(\omega) = f(\mathbf{X}_{<t}(\omega), \varepsilon(\omega)) \quad (12)$$

is an ODE.

Note that  $\mathbf{X}_t$  in Eq. 11 is a random variable and characterizes a DSP  $\mathbf{X} : T \times \Omega \rightarrow \mathbb{R}^n$  induced by  $\varepsilon$ . In this sense, we say that  $\mathbf{X}$  is a solution of Eq. 11. Equivalently, we say that  $\mathbf{X}$  is a *solution* of Eq. 11 if Eq. 12 is satisfied for *almost all*  $\omega \in \Omega$ .

**Example 1 (RDE).** The system described by

$$\begin{cases} X_t = a(\Omega)X_{t-1} + b(\Omega) \\ X_0 = X_0(\Omega) \end{cases} \quad (13)$$

represents a first-order linear RDE equipped with an initial condition for  $X_0$ , in which the stochasticity of  $\omega$  generates a distribution over  $X_0$  and over the parameters of the equation  $a, b$ . The general solution of Equation 13 can be found by recursive substitution, obtaining  $X_t(\omega) = a(\omega)^t X_0(\omega) + b(\omega) \sum_{i=0}^{t-1} a(\omega)^i$ .

<sup>8</sup>In (Bongers, Blom, and Mooij 2018),  $\varepsilon$  is regarded as a stochastic process that converges eventually or asymptotically to a time-independent random variable. In this work, simplifying the concept, we consider it as a random variable throughout the whole process.

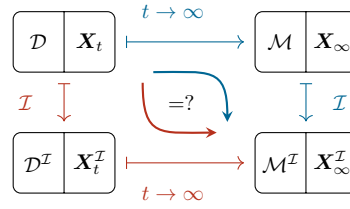


Figure 7: Illustration of the relationship between RDEs & SCMs and the effect of causal interventions on them. Applying equilibration (here denoted by  $t \rightarrow \infty$ ) before or after intervention does not change the final resulting distribution  $\mathbf{X}_\infty^I$ , i.e., the diagram commutes. For SDEs, when variables are localized in times, commutation is not preserved, that is  $(\mathbf{X}_\infty)^{\mathcal{I}\mathcal{M}} \neq (\mathbf{X}^{\mathcal{I}\mathcal{D}})_\infty$ .

### A.2 Stochastic Processes Equilibration

Let  $\mathbf{X}$  be a DSP. We say that  $\mathbf{X}$  (*strongly*) *equilibrates* if  $\mathbf{X}_t$  converges to a random variable  $\mathbf{X}_\infty$  for  $t \rightarrow \infty$  almost surely, i.e.,

$$\mathbb{P}(\limsup_{t \rightarrow \infty} \{\omega \in \Omega : |\mathbf{X}_t(\omega) - \mathbf{X}_\infty(\omega)| > \varepsilon\}) = 0 \quad \forall \varepsilon > 0,$$

denoted by  $\mathbf{X}_t \xrightarrow{a.s.} \mathbf{X}_\infty$ . We call  $\mathbf{X}_\infty$  the *equilibrium state* of  $\mathbf{X}$ . Moreover, we say that  $\mathbf{X}$  *weakly equilibrates* if  $\mathbf{X}_t$  converges in distribution to a random variable  $\mathbf{X}_\infty$ , i.e., for all  $x$  for which  $F_{\mathbf{X}}$  (the CDF of  $\mathbf{X}$ ) is continuous,

$$\lim_{t \rightarrow \infty} F_{\mathbf{X}_t}(x) = F_{\mathbf{X}_\infty}(x), \quad \text{denoted by } \mathbf{X}_t \xrightarrow{d} \mathbf{X}_\infty.$$

In general,  $\mathbf{X}_t \xrightarrow{a.s.} \mathbf{X}_\infty \Rightarrow \mathbf{X}_t \xrightarrow{d} \mathbf{X}_\infty$ .

**Remark 1.** If  $\mathbf{X}$  is a solution of an RDE, almost sure convergence is achieved if and only if, for almost all  $\omega \in \Omega$ , the solution of the ordinary difference equation (ODE) in Equation 12 converges asymptotically to a fixed value  $\mathbf{X}_\infty(\omega)$ . On the other hand, a DSP that is a solution of a SDE (for convenience, we recall Equation 2:  $\mathbf{X}_t = \mathbf{f}(\mathbf{X}_{<t}) + \mathbf{g}(\mathbf{X}_{<t}) \odot \varepsilon_t$ ) cannot equilibrate unless the term  $\mathbf{g}(\mathbf{X}_{<t})$  converges as  $t \rightarrow \infty$  to 0, thereby transforming the equation into a RDE. Apart from this scenario, no solutions of a SDE can strongly equilibrate.

**Example 2 (RDE equilibration).** Consider example 1. Assuming  $a(\omega) < 1 \quad \forall \omega \in \Omega$ ,

$$X_t \xrightarrow{a.s.} X_\infty = b(\Omega) \sum_{i=0}^{\infty} a(\Omega)^i = \frac{b(\Omega)}{1 - a(\Omega)}.$$

### A.3 Equilibration as a map from RDEs to SCMs

The process equilibration allows defining a map that associates each RDE with an SCM. Furthermore, this map preserves the semantic of intervention, in the same sense of §3.2. Visually, the diagram in Fig. 7 commutes, i.e., applying equilibration before or after intervention doesn't change the resulting  $\mathbf{X}_\infty^I$ .

Consider a Simple RDE  $\mathcal{D}$  and its solution  $\mathbf{X}$ . Let  $\mathbf{X}_\infty$  be the random variable which  $\mathbf{X}$  equilibrates to. Then it is

possible to associate an SCM  $\mathcal{M}_{\mathcal{D}} = (\mathbf{F}, \mathbf{E})$  where  $\mathbf{E} = \varepsilon_{\mathcal{D}}$  and  $\mathbf{F}$  is defined through the equilibrium relation

$$\mathbf{X}_{\infty} = f_{\mathcal{D}}(\mathbf{X}_{\infty}(\cdot), \mathbf{E}) = \tilde{f}(\mathbf{X}_{\infty}, \mathbf{E}), \quad (14)$$

where  $\mathbf{X}_{\infty}(t, \cdot) = \mathbf{X}_{\infty} \forall t$  is the constant stochastic process associated with  $\mathbf{X}_{\infty}$ . In other words,  $\mathcal{M}_{\mathcal{D}}$  fully inherits the functional relationships of  $\mathcal{D}$ , substituting dynamic variables with their stationary counterparts. A proof for the general case in continuous-time can be found in (Bongers, Blom, and Mooij 2018). The discrete-time variant follows directly by applying methods of numerical approximation (Hildebrand 1987; Jornet 2023).

#### A.4 Equilibration as a map from SDEs to SCMs

Associating an SDE with an SCM in non-linear settings involves two steps. The first concerns the convergence conditions of the dynamical system to a stationary (observational) distribution. The second step involves constructing the mapping between interventions in the two different models and proving their equivalence. In this work, we address the first point. As for the second, a formal treatment of the nonlinear case has yet to be completed. While intuitively the existence of an appropriate SCM seems more than reasonable, its explicit characterization requires mathematical tools beyond the scope of this work. We intend to tackle this step in future research.

**Existence of an observational limit distribution** Several works discuss the existence and uniqueness of a limit distribution for stochastic systems (Arnold et al. 1995; Bhat-tacharya and Majumdar 2003; Łoskot and Rudnicki 1995). Here, we adapt the following theorem from (Lasota and Mackey 1989) to our formulation in Eq. 2:

**Theorem 2.** [Adapted Eq. 2 from (Lasota and Mackey 1989)] Consider a SDE<sup>9</sup> described by

$$\mathbf{X}_t = f(\mathbf{X}_{t-1}) + g(\mathbf{X}_{t-1}) \odot \varepsilon_t.$$

If the following conditions hold: i)  $f, g : \mathcal{X} \rightarrow \mathcal{X}$  are continuous in  $\mathbf{X}_{t-1}$ , and  $\mathcal{X} \subset \mathbb{R}^d$  is closed; ii)  $\varepsilon_t$  is i.i.d. white noise; and iii) for every  $t$ ,

$$(iii.1) \quad \forall x, y \in \mathcal{X}, x \neq y \\ \mathbb{E}[\|f(x) + g(x) \odot \varepsilon_t - f(y) - g(y) \odot \varepsilon_t\|] < \|x - y\|$$

$$(iii.2) \quad \forall x \in \mathcal{X} \\ \mathbb{E}[\|f(x) + g(x) \odot \varepsilon_t\|^2] \leq \alpha \|x\|^2 + \beta, \alpha < 1,$$

where  $\|\cdot\|$  is the Euclidean norm in  $\mathbb{R}^d$ . Then, there exists a unique invariant distribution  $p(\mathbf{X}_{\infty})$  to which  $p(\mathbf{X}_t)$  converges as  $t \rightarrow \infty$ , regardless of the initial state  $\mathbf{X}_0$ .

<sup>9</sup>Thm. 2 considers Markovian systems, while our formulation allows for  $f$  and  $g$  to depend on multiple past states. As long as the states considered are finite in number, i.e.,  $s$  depends on  $\mathbf{X}_{t-1}, \mathbf{X}_{t-2}, \dots, \mathbf{X}_{t-p}$ ,  $p < \infty$ , it is always possible to represent the system as if it were Markovian, through the transformation  $\mathbf{Z}_t := [\mathbf{X}_t, \mathbf{X}_{t-1}, \dots, \mathbf{X}_{t-p+1}]$ . Given this fact, for ease of exposition, we will consider strictly Markovian systems in the discussion.

#### Rediscussing Thm. 2 in terms of Lipschitz continuity

For a more intuitive interpretation of Thm. 2, we show that condition (iii) holds under Lipschitz continuity<sup>10</sup> of  $f$  and  $g$ . Given  $f, g : \mathbb{R}^d \rightarrow \mathbb{R}^d$  Lipschitz continuous with Lipschitz constants  $L_f, L_g$ , we want to find sufficient conditions on  $L_f$  and  $L_g$  such that, for every fixed  $x, y$ ,

$$(1) \quad \mathbb{E}[\|f(x) + g(x) \odot \varepsilon - f(y) - g(y) \odot \varepsilon\|] < \|x - y\|. \\ (2) \quad \mathbb{E}[\|f(x) + g(x) \odot \varepsilon\|^2] \leq \alpha \|x\|^2 + \beta, \alpha < 1.$$

$\varepsilon$  being a random vector s.t. each of its component satisfy  $\mathbb{E}[\varepsilon] = 0, \mathbb{E}[\|\varepsilon\|^2] < \infty$ . For (1) we calculate

$$\begin{aligned} \mathbb{E}[\|f(x) + g(x) \odot \varepsilon - f(y) - g(y) \odot \varepsilon\|] &\leq \\ \|f(x) - f(y)\| + \|g(x) - g(y)\| \mathbb{E}[\|\varepsilon\|] &\leq \\ L_f \|x - y\| + L_g \|x - y\| \mathbb{E}[\|\varepsilon\|] &= \\ (L_f + L_g \mathbb{E}[\|\varepsilon\|]) \|x - y\| &< \|x - y\| \\ \iff \boxed{L_f + L_g \mathbb{E}[\|\varepsilon\|] < 1} \end{aligned}$$

The same procedure for (2) yields

$$\begin{aligned} \mathbb{E}[\|f(x) + g(x) \odot \varepsilon\|^2] &= \\ \mathbb{E}[\|f(x)\|^2] + \mathbb{E}[\|g(x) \odot \varepsilon\|^2] &= \{\hat{f}(x) := f(x) - f(0)\} \\ \mathbb{E}[\|\hat{f}(x) + f(0)\|^2] + \mathbb{E}[\|\hat{g}(x) \odot \varepsilon + g(0) \odot \varepsilon\|^2] &\leq \\ L_f^2 \|x\|^2 + 2|\langle \hat{f}(x), f(0) \rangle| + \|f(0)\|^2 + & \\ L_g^2 \|x\|^2 \sigma^2 + 2|\langle \hat{g}(x), g(0) \rangle| \sigma^2 + \|g(0)\|^2 \sigma^2 &\leq \{\sigma^2 := \mathbb{E}[\|\varepsilon\|^2]\} \\ (L_f^2 + L_g^2 \sigma^2) \|x\|^2 + 2(L_f \|f(0)\| + L_g \|g(0)\| \sigma^2) \|x\| + & \\ \|f(0)\|^2 + \|g(0)\|^2 \sigma^2 =: a \|x\|^2 + m \|x\| + b. \end{aligned}$$

Observing that every polynomial  $ax^2 + mx + b$  with  $a > 0$  can be bounded above by  $\alpha x^2 + \beta$  assuming  $\alpha > a$  and provided that  $\beta$  is sufficiently large, we finally obtain

$$a \|x\|^2 + m \|x\| + b \leq \alpha x^2 + \beta, \alpha < 1 \\ \iff \boxed{L_f^2 + L_g^2 \mathbb{E}[\|\varepsilon\|^2] < 1}$$

In the simple case in which  $g \equiv 1$ , we obtain the inequality  $L_f < 1$ , i.e.,  $f$  is a contraction. Condition (2) disappears, as  $L_f^2 < L_f < 1$ . In the general case, we interpret  $f$  as a contraction map on  $\mathbf{X}_{\infty}$  and  $g \odot \varepsilon_t$  as a diffusion process. The equilibrium between these processes generates the invariant distribution.

## B Vector Autoregressive Models

### B.1 Properties

A VAR process  $\mathbf{X}_t$  is stable if all roots of the determinantal polynomial of the VAR operator are outside the complex unit circle. This condition can be formally expressed as:

$$\det(I_K - \mathbf{A}_1 z - \dots - \mathbf{A}_p z^p) \neq 0 \quad \forall z \in \mathbb{C}, |z| \leq 1, \quad (15)$$

where  $\mathbb{C}$  denotes the set of complex numbers. The stability condition ensures that the process is stationary (Lütkepohl

<sup>10</sup>A function  $f$  is Lipschitz with constant  $L$  if for all  $x, y$ , it holds that  $\|f(x) - f(y)\| \leq L \|x - y\|$ .

2005). Consequently, a stable VAR( $p$ ) process  $\mathbf{X}_t$  is stationary.

In (Wold 1938), the author introduced the Wold decomposition Theorem, which states that every covariance-stationary time series  $\mathbf{X}_t$  can be written as the sum of two uncorrelated processes as  $\mathbf{X}_t = \mathbf{Z}_t + \mathbf{Y}_t$  where  $\mathbf{Z}_t$  is a deterministic component that can be forecast perfectly from its past, and  $\mathbf{Y}_t$  is a purely stochastic process with an infinite-order Moving Average (MA) representation:

$$\mathbf{Y}_t = \sum_{i=0}^{\infty} \Phi_i \mathbf{u}_{t-i}. \quad (16)$$

Suppose the  $\Phi_i$  are absolutely summable and that there exists an operator  $A(L)$  with absolutely summable coefficient matrices satisfying  $A(L)\Phi(L) = I_K$ . Then  $\Phi(L)$  is invertible with  $\Phi(L)^{-1} = A(L)$  and  $\mathbf{Y}_t$  can be approximated arbitrarily well by a finite-order VAR( $p$ ) with  $p$  sufficiently large, and  $A(L) = I - \mathbf{A}_1 L - \dots - \mathbf{A}_p L^p$ , where  $I$  is the identity matrix.

In particular, the matrices  $\Phi_i$  of a VAR( $p$ ) model can be calculated by recursively applying the formula

$$\Phi_0 = I, \quad \Phi_i = \sum_{j=1}^i \Phi_{i-j} \mathbf{A}_j, \quad \text{where } \mathbf{A}_j = 0 \text{ for } j > p. \quad (17)$$

**Remark.** Consider the model  $A(L)\mathbf{X}_t = \boldsymbol{\nu} + \mathbf{u}_t$ , where  $\boldsymbol{\nu}$  is a (constant) intercept term. Using Wold's Theorem, we can express it by linearity of  $\Phi$  as  $\mathbf{X}_t = \Phi(L)\boldsymbol{\nu} + \Phi(L)\mathbf{u}_t$ . Noting that  $L\boldsymbol{\nu} = \boldsymbol{\nu}$ , we obtain

$$\mathbf{X}_t = \boldsymbol{\mu} + \Phi(L)\mathbf{u}_t$$

where  $\boldsymbol{\mu} = \Phi(1)\boldsymbol{\nu} := \sum_{l=0}^{\infty} \Phi_l \boldsymbol{\nu}$ . Due to the invertibility of  $\Phi(L)$ , we can express the same relation through  $\boldsymbol{\nu} = \Phi(1)^{-1}\boldsymbol{\mu} = A(1)\boldsymbol{\mu} = [1 - \mathbf{A}_1 - \dots - \mathbf{A}_p]\boldsymbol{\mu}$ . From this observation, we automatically obtain the equality

$$\sum_{l=0}^{\infty} \Phi_l = \Phi(1) = A(1)^{-1} = [1 - \mathbf{A}_1 - \dots - \mathbf{A}_p]^{-1}. \quad (18)$$

## B.2 Proof of Thm. 1 - From VARs to SCMs (§4.1)

Consider the  $MA(\infty)$  representation of  $\mathbf{X}_t$  (since we can always apply a translation to it without modifying the dynamic of the stochastic part, let's assume for simplicity that  $\mathbb{E}[\mathbf{X}_t] = 0$ ):

$$\mathbf{X}_t = \sum_{l=0}^{\infty} \Phi_l \mathbf{u}_{t-l}.$$

To capture the long-run relationships of the process, we apply the transformation

$$\mathcal{T} : \mathbf{X}_t \mapsto \mathbf{Z}_t = \frac{1}{\sqrt{t}} \sum_{i=1}^t \mathbf{X}_i, \quad (19)$$

By examining the equilibration  $\mathbf{Z}_t \rightarrow \mathbf{Z}_{\infty}$ , we can link a stable VAR( $p$ ) process to the following SCM:

$$\tilde{\mathbf{X}} = \tilde{\mathbf{A}}\tilde{\mathbf{X}} + \tilde{\mathbf{u}}, \quad \text{where } \tilde{\mathbf{A}} := \left[ \sum_{i=1}^p \mathbf{A}_i \right]$$

Here, we outline the proof:

$$\begin{aligned} \lim_{t \rightarrow \infty} \mathbf{Z}_t &= \lim_{t \rightarrow \infty} \frac{1}{\sqrt{t}} \sum_{i=1}^t \sum_{l=0}^{\infty} \Phi_l \mathbf{u}_{i-l} = \\ &\text{(by a.s. absolute convergence)} \\ &= \lim_{t \rightarrow \infty} \frac{1}{\sqrt{t}} \sum_{l=0}^{\infty} \sum_{i=1}^t \Phi_l \mathbf{u}_{i-l} = \\ &= \lim_{t \rightarrow \infty} \sum_{l=0}^{\infty} \Phi_l \frac{1}{\sqrt{t}} \sum_{i=1}^t \mathbf{u}_{i-l} = \\ &\text{(by dominated convergence)} \\ &= \sum_{l=0}^{\infty} \Phi_l \lim_{t \rightarrow \infty} \frac{1}{\sqrt{t}} \sum_{i=1}^t \mathbf{u}_{i-l} = \\ &\text{(by central limit theorem)} \\ &\stackrel{d}{=} \left[ \sum_{l=0}^{\infty} \Phi_l \right] \tilde{\mathbf{u}}, \quad \tilde{\mathbf{u}} \sim \mathcal{N}(0, \Sigma_{\mathbf{u}}) = \quad (*) \\ &= \Phi(1)\tilde{\mathbf{u}} = A(1)^{-1}\tilde{\mathbf{u}} = [1 - \mathbf{A}_1 - \dots - \mathbf{A}_p]^{-1} \tilde{\mathbf{u}}, \end{aligned}$$

that is

$$\begin{aligned} \mathbf{Z}_{\infty} &\stackrel{d}{=} A(1)^{-1} \tilde{\mathbf{u}}, \quad \text{or equivalently} \\ \mathbf{Z}_{\infty} &\stackrel{d}{=} [\mathbf{A}_1 + \dots + \mathbf{A}_p] \mathbf{Z}_{\infty} + \tilde{\mathbf{u}} \quad \square \end{aligned} \quad (20)$$

For an alternative proof of (\*) see (Hamilton 1994, 194) and (Anderson 1994, 429), from which we report the main statement:

**Theorem 3.** (Anderson 1994, 429) Let  $\mathbf{X}$  be a DSP defined by

$$\mathbf{X}_t = \boldsymbol{\mu} + \sum_{l=0}^{\infty} \Phi_l \mathbf{u}_{t-l} \quad (21)$$

such that  $\mathbf{u}_t$  is white noise and  $\sum_{l=0}^{\infty} |\Phi_l| < \infty$ . Then

$$\mathbf{Z}_t = \frac{1}{\sqrt{t}} \sum_{i=1}^t (\mathbf{X}_i - \boldsymbol{\mu}) \xrightarrow{d} \mathcal{N}(0, \sum_{i=-\infty}^{\infty} \gamma_i) \quad \text{as } t \rightarrow \infty,$$

where  $\gamma_i$  represents the autocovariance  $\text{Var}(\mathbf{X}_t, \mathbf{X}_{t-i})$ .

Exploiting the i.i.d assumption for  $\mathbf{u}_t$ ,  $\gamma_i$  admits the representation

$$\gamma_i = \sum_{l=0}^{\infty} \Phi_{l+i} \Sigma_{\mathbf{u}} \Phi_l' = \sum_{k=0}^{\infty} \sum_{l=0}^{\infty} \delta_{k, l+i} \Phi_k \Sigma_{\mathbf{u}} \Phi_l'.$$

Using  $\sum_{i=-\infty}^{\infty} \delta_{i,j} = 1 \forall j$ , we rewrite

$$\begin{aligned}
\sum_{i=-\infty}^{\infty} \gamma_i &= \sum_{i=-\infty}^{\infty} \sum_{k=0}^{\infty} \sum_{l=0}^{\infty} \delta_{k,l+i} \Phi_k \Sigma_{\mathbf{u}} \Phi_l' = \\
&\text{(absolute convergence)} \\
&= \sum_{k=0}^{\infty} \sum_{l=0}^{\infty} \sum_{i=-\infty}^{\infty} \delta_{k,l+i} \Phi_k \Sigma_{\mathbf{u}} \Phi_l' = \\
&= \sum_{k=0}^{\infty} \sum_{l=0}^{\infty} \Phi_k \Sigma_{\mathbf{u}} \Phi_l' = \\
&= \left[ \sum_{k=0}^{\infty} \Phi_k \right] \Sigma_{\mathbf{u}} \left[ \sum_{l=0}^{\infty} \Phi_l' \right] = \Phi(1) \Sigma_{\mathbf{u}} \Phi(1)', \tag{22}
\end{aligned}$$

that is compatible with Eq. 20. Additionally, it is worth noting that given a positive definite covariance matrix  $\Sigma_{\mathbf{Z}}$  and a fixed order of variables in  $\mathbf{Z}$ , Cholesky decomposition (Lütkepohl 2005) guarantees the existence and uniqueness of a triangular matrix  $L$  such that  $\Sigma_{\mathbf{Z}} = LL'$ . The same holds for LDL decomposition (Lütkepohl 2005), namely  $\Sigma_{\mathbf{Z}} = LDL'$ . Setting  $L = \Phi(1)$  and  $D = \Sigma_{\mathbf{u}}$ , we can deduce Eq. 20 from Thm. 3.

**Equilibration commutes with additive intervention** We show that applying the same additive intervention on the VAR and its associated SCM yields the same interventional distribution. We start by studying the long term effect of the additive term  $\mathbf{F}$  over the VAR model:

$$\begin{aligned}
A(L)\mathbf{X}_t &= \mathbf{u}_t + \mathbf{F} \Rightarrow \mathbf{X}_t = \Phi(L)\mathbf{u}_t + \Phi(1)\mathbf{F}, \\
\text{where } \Phi(1)\mathbf{F} &= \sum_{l=0}^{\infty} \Phi_l \mathbf{F}.
\end{aligned}$$

By applying  $\mathcal{T}$  (Eq. 19) and Eq. 20, we obtain

$$\mathbf{Z}_{\infty}^{\mathcal{I}} = \Phi(1)\tilde{\mathbf{u}} + \Phi(1)\mathbf{F}.$$

Using Thm. 1, we study the same intervention of the associated SCM:

$$\begin{aligned}
\tilde{\mathbf{X}} &= \tilde{\mathbf{A}}\tilde{\mathbf{X}} + \tilde{\mathbf{u}} + \mathbf{F} \Rightarrow \\
[I - \tilde{\mathbf{A}}]\tilde{\mathbf{X}} &= \tilde{\mathbf{u}} + \mathbf{F} \Rightarrow \\
\tilde{\mathbf{X}} &= [I - \tilde{\mathbf{A}}]^{-1}\tilde{\mathbf{u}} + [I - \tilde{\mathbf{A}}]^{-1}\mathbf{F}.
\end{aligned}$$

The correspondence follows directly from  $\Phi(1) = \mathbf{A}(1)^{-1} = [I - \tilde{\mathbf{A}}]^{-1}$ .

**Equilibration commutes with forcing intervention** We report Eq. 10 for clarity of exposition:

$$\mathbf{A}(L)\mathbf{X}_t = \boldsymbol{\nu} + \mathbf{u}_t + \mathbb{I}(t \geq t_0)\mathbf{F} \odot (\hat{\mathbf{X}} - \mathbf{X}_t)$$

We can rewrite the equation by shifting the term  $\mathbf{F} \odot \mathbf{X}_t$  to the left, reformulating it in matrix form  $\mathbf{F}_{diag}\mathbf{X}_t$ , and obtaining  $[\mathbf{A}(L) + \mathbf{F}_{diag}]\mathbf{X}_t = \boldsymbol{\nu} + \mathbf{u}_t + \mathbb{I}(t \geq t_0)\mathbf{F} \odot \hat{\mathbf{X}}$ . By

defining  $\mathbf{A}_{\mathcal{I}}(L) := \mathbf{A}(L) + \mathbf{F}_{diag}$  and  $\tilde{\mathbf{F}} := \mathbf{F} \odot \hat{\mathbf{X}}$ , we obtain  $\mathbf{A}_{\mathcal{I}}(L)\mathbf{X}_t = \boldsymbol{\nu} + \mathbf{u}_t + \mathbb{I}(t \geq t_0)\tilde{\mathbf{F}}$ , which is again an additive intervention, but on the intervened dynamic. For this reason, we can prove the case  $\hat{\mathbf{X}} = \mathbf{0}$  and directly applying the result of additive intervention afterwards. By applying  $\mathcal{T}$  (Eq. 19) and equilibrating, we obtain

$$\mathbf{Z}_{\infty}^{\mathcal{I}} = \mathbf{A}_{\mathcal{I}}(1)^{-1}\tilde{\mathbf{u}}$$

Consider the analogue of forcing intervention over an SCM:

$$\tilde{\mathbf{X}} = \tilde{\mathbf{A}}\tilde{\mathbf{X}} + \tilde{\mathbf{u}} - \mathbf{F} \odot \tilde{\mathbf{X}}, \quad \text{where we fixed } \hat{\mathbf{X}} = \mathbf{0}.$$

We can rewrite it as  $[I - \tilde{\mathbf{A}} + \mathbf{F}_{diag}]\tilde{\mathbf{X}} = \tilde{\mathbf{u}}$ , that is  $\mathbf{A}_{\mathcal{I}}(1)\tilde{\mathbf{X}} = \tilde{\mathbf{u}} \Rightarrow \tilde{\mathbf{X}} = \mathbf{A}_{\mathcal{I}}(1)^{-1}\tilde{\mathbf{u}}$ .  $\square$

### B.3 Stability of forcing intervention is not guaranteed: an example

$\mathcal{I}_f$  perturbs the system dynamics by modifying the operator  $\mathbf{A}(L)$ . Specifically, by shifting the term  $\mathbf{F} \odot \mathbf{X}_t$  to the left of the equation and rewriting it in matrix form as  $\mathbf{F}_{diag}\mathbf{X}_t$ , we obtain  $\mathbf{A}_{\mathcal{I}}(L) := \mathbf{A}(L) + \mathbf{F}_{diag}$ . Hence, the stability of the intervened system is not guaranteed, and it is necessary to verify that all the eigenvalues of  $\mathbf{A}_{\mathcal{I}}(L)$  are still inside the unit circle.

When applying a forcing intervention, the intensity of  $\mathbf{F}$  can play an important role. To show this, consider the toy model described by the VAR(1) equation

$$\begin{bmatrix} X^{(1)} \\ X^{(2)} \end{bmatrix}_t = \sqrt{2} \begin{bmatrix} 0 & -0.5 \\ 0.5 & 1 \end{bmatrix} \begin{bmatrix} X^{(1)} \\ X^{(2)} \end{bmatrix}_{t-1} + \begin{bmatrix} \boldsymbol{\varepsilon}^{(1)} \\ \boldsymbol{\varepsilon}^{(2)} \end{bmatrix}_t. \tag{23}$$

the roots of  $\det(I - \mathbf{A}_1 z)$  are  $z_{1,2} = \sqrt{2} > 1$ , indicating that the system is stable. Applying  $\mathcal{I}_f$  to component  $X^{(1)}$ , we need to examine

$$\det \left( \begin{bmatrix} 1 + F & 0 \\ 0 & 1 \end{bmatrix} - \sqrt{2} \begin{bmatrix} 0 & -0.5 \\ 0.5 & 1 \end{bmatrix} z \right)$$

which have roots  $z_{1,2} = \sqrt{2}(1 + F \pm \sqrt{F^2 + F})$ . It is easy to verify that for  $F = 1$ , one root is less than 1, and thus the model is no longer stable. On the other hand, intervening on  $X^{(2)}$  preserves stability regardless of  $F$  intensity; the same procedure yields  $z_{1,2} = \sqrt{2}(1 \pm \sqrt{-F})$ , so that  $|z_{1,2}| \geq \sqrt{2} > 1 \forall F > 0$ .

It is possible to identify sufficient conditions for  $\mathcal{D}$  to be always stable under intervention. In particular, it is easy to see that if all matrices  $\mathbf{A}_i$  of the model are strictly lower triangular, and thus  $\mathcal{G}_{\mathcal{D}}$  is acyclic,  $\mathbf{X}_t$  has a finite Moving Average representation. This property is preserved by any intervention  $\mathcal{I}_f$ . Acyclicity can be weakened to allow *self-loops*.

**Stable VARs with at most self-loops are interventionally stable** Given a VAR model such that all its matrices  $\mathbf{A}_i$  are (non-strictly) lower triangular, the stability of the intervened system directly follows from the stability of the observational one. To verify this, note that the determinantal polynomial of the model

$$\det(I - \mathbf{A}_1 z - \dots - \mathbf{A}_p z^p) \quad (\text{as in Eq. 15})$$

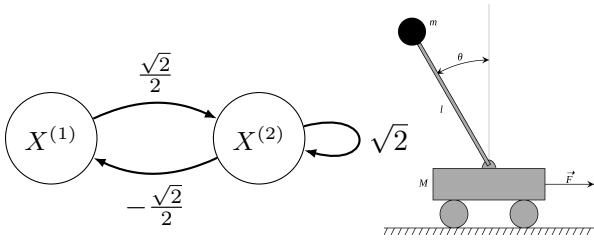


Figure 8: (left) A simple model that lacks interventional stability:  $X^{(1)}$  functions as a stabilizer for  $X^{(2)}$ , which exhibits a divergent dynamic. Intervening on  $X^{(1)}$  disrupts the negative feedback loop, making the system unstable. (right) A concrete example of the model from control theory is the inverted pendulum:  $X^{(1)}$  is the position of the cart, while  $X^{(2)}$  is the angle  $\theta$ ; fixing the cart makes the system unstable, i.e., the pendulum falls. As a practical example, consider optimal control applications to nuclear reactors management (Edwards, Lee, and Ray 1992).

reduces to the product of diagonal terms since all matrices are triangular, and each  $i$ -th root satisfies the relation  $p_i(z) = 1 - \mathbf{A}_1[i, i]z - \dots - \mathbf{A}_p[i, i]z^p = 0$ . Observing that  $p_i(0) = 1 > 0$  and considering the root with the smallest norm  $z_{min}$ , using the continuity of  $p_i$ , we can deduce that  $p_i(z) > 0 \forall z$  such that  $|z| < |z_{min}|$ . Intervening on component  $i$  yields  $\tilde{p}_i(z) = p_i(z) + F$ , from which we can conclude  $\tilde{p}_i(z) > F > 0$  for all  $z$  with norm lower than  $z_{min}$ , and in particular for all those within the unit circle.

## C Answering causal queries in practice

In this section, we report the actual execution of the procedures used in our work to calculate forecasting (C.1), interventional forecasting (C.2), and retrospective counterfactuals (C.3).

### C.1 Forecasting

Forecasting is one of the main objectives of time series analysis in general (Montgomery, Jennings, and Kulahci 2015). We discuss predictors based on VAR processes that minimize the Mean Square Error (MSE).

**Objective** Suppose we have a time series  $\mathbf{X}_t$  up to time  $t_0$  and we want to predict the state of the system after  $h$  steps  $\mathbf{X}_{t_0+h}$ . We call a predictor for this quantity the  $h$ -steps predictor. In particular, the optimal predictor with respect to MSE is

$$\mathbb{E}[\mathbf{X}_{t_0+h} | \mathbf{X}_{\leq t_0}].$$

The optimality of the expected value relies on the assumption that  $\mathbf{u}_t$  in Eq. 3 is *i.i.d. white noise*. For a VAR(p) as in Eq. 3, the optimal  $h$ -step predictor can be evaluated by recursively applying

$$\begin{aligned} \mathbb{E}[\mathbf{X}_{t+k} | \mathbf{X}_{\leq t}] &= \boldsymbol{\nu} + \mathbf{A}_1 \mathbb{E}[\mathbf{X}_{t+k-1} | \mathbf{X}_{\leq t}] + \\ &\dots + \mathbf{A}_p \mathbb{E}[\mathbf{X}_{t+k-p} | \mathbf{X}_{\leq t}], \end{aligned} \quad (24)$$

where  $\mathbb{E}[\mathbf{X}_{t'} | \mathbf{X}_{\leq t}] = \mathbf{X}_{t'}$  if  $t' \leq t$ . In other words, it is possible to forecast all subsequent values of  $\mathbf{X}_{t_0}$  by applying

the original equation of the VAR without considering the noise  $\mathbf{u}_t$ . For example, considering the 1-step predictor, we get

$$\mathbb{E}[\mathbf{X}_{t_0+1} | \mathbf{X}_{\leq t_0}] = \boldsymbol{\nu} + \mathbf{A}_1 \mathbf{X}_{t_0} + \dots + \mathbf{A}_p \mathbf{X}_{t_0+1-p}.$$

Similarly, by exploiting the possibility of recursively applying Eq. 24, we obtain the estimate of the forecast error covariance (or MSE) matrix as

$$\Sigma_{\mathbf{X}}(k) = \sum_{i=0}^{h-1} \Phi_i \Sigma_{\mathbf{u}} \Phi_i'.$$

Note that each term in the sum is a positive definite matrix, and consequently, the MSE matrix is monotonically non-decreasing.  $\Sigma_{\mathbf{X}}(k)$  approaches the covariance matrix of  $\mathbf{X}_t$ ,  $\Sigma_{\mathbf{X}}$ , for  $k \rightarrow \infty$ . In fact, the optimal long-range forecast  $h \rightarrow \infty$  is just the process mean. In other words, the past of the process contains no information on the development of the process in the distant future.

### C.2 Interventional Forecasting

Consider again a VAR(p) model described by Eq. 3 and suppose an intervention is applied to the system at time  $t_0$ . We report the procedure for performing interventional forecasts for additive and forcing interventions separately.

**Additive intervention** The model equations are modified only by adding the term  $\mathbf{F}$ , consequently, Eq. 24 simply becomes

$$\begin{aligned} \mathbb{E}[\mathbf{X}_{t+k} | \mathbf{X}_{\leq t}] &= \hat{\boldsymbol{\nu}} + \mathbf{A}_1 \mathbb{E}[\mathbf{X}_{t+k-1} | \mathbf{X}_{\leq t}] + \\ &\dots + \mathbf{A}_p \mathbb{E}[\mathbf{X}_{t+k-p} | \mathbf{X}_{\leq t}], \quad \text{where } \hat{\boldsymbol{\nu}} = \boldsymbol{\nu} + \mathbf{F} \end{aligned} \quad (25)$$

The MSE matrix remains unchanged, as both  $\Sigma_{\mathbf{u}}$  and all the matrices (and consequently the matrices  $\Phi_i$ , see Eq. 17) are not modified.

Alternatively, exploiting the linearity of the predictor, it is possible to directly estimate the expected causal effect at time  $h$  through

$$\text{CE}_{t_0+h} = \sum_{l=0}^h \Phi_l \mathbf{F},$$

and add this quantity to the observational forecast. The resulting interventional forecast is equivalent.

**Forcing intervention** In this case, the intervention modifies the matrices  $\mathbf{A}_i$  of the process, and the procedure is more complex. Let us proceed step by step. The intervened model is described by (see Eq. 10)

$$\begin{aligned}
\mathbf{X}_t &= \boldsymbol{\nu} + \mathbf{F} \odot (\hat{\mathbf{X}} - \mathbf{X}_t) + \sum_{i=1}^p \mathbf{A}_i \mathbf{X}_{t-i} + \mathbf{u}_t \\
\Rightarrow [I + \mathbf{F}_{diag}] \mathbf{X}_t &= \boldsymbol{\nu} + \mathbf{F} \odot \hat{\mathbf{X}} + \sum_{i=1}^p \mathbf{A}_i \mathbf{X}_{t-i} + \mathbf{u}_t \\
\text{where } \mathbf{F}_{diag} &:= I \cdot \mathbf{F} \\
\Rightarrow [I + \mathbf{F}_{diag}] \mathbf{X}_t &= \hat{\boldsymbol{\nu}} + \sum_{i=1}^p \mathbf{A}_i \mathbf{X}_{t-i} + \mathbf{u}_t \\
\text{where } \hat{\boldsymbol{\nu}} &:= \boldsymbol{\nu} + \mathbf{F} \odot \hat{\mathbf{X}} \\
\Rightarrow \mathbf{X}_t &= [I + \mathbf{F}_{diag}]^{-1} \left( \hat{\boldsymbol{\nu}} + \sum_{i=1}^p \mathbf{A}_i \mathbf{X}_{t-i} + \mathbf{u}_t \right) \\
\Rightarrow \mathbf{X}_t &= \tilde{\boldsymbol{\nu}} + \sum_{i=1}^p \tilde{\mathbf{A}}_i \mathbf{X}_{t-i} + \tilde{\mathbf{u}}_t,
\end{aligned} \tag{26}$$

where  $\tilde{\boldsymbol{\nu}}, \tilde{\mathbf{A}}_i, \tilde{\mathbf{u}}_t$  are the results of left-multiplying their respective elements by  $[I + \mathbf{F}_{diag}]^{-1}$ .

The resulting equation has the form of a standard VAR(p) model, so we can apply the forecasting exactly as in App. C.1. The same applies to the MSE matrix, calculated using the modified matrices  $\Sigma_{\tilde{\mathbf{u}}}$  and  $\tilde{\Phi}_i$ .

Unlike the additive intervention, there is no way to directly calculate the causal effect. The estimate is therefore obtained through the difference.

$$CE_{t_0+h} = \mathbb{E}[\tilde{\mathbf{X}}_{t_0+h} | \mathbf{X}_{\leq t}] - \mathbb{E}[\mathbf{X}_{t_0+h} | \mathbf{X}_{\leq t}],$$

that is *the difference between the interventional forecast and the observational one*.

### C.3 Retrospective Counterfactuals

In the *ladder of causality* (Pearl 2009; Bareinboim et al. 2022), counterfactual statements belong to the last level, distinct from the interventional level, and a mature causal model should be able to address both. Embracing this perspective, we show how counterfactual queries can be formulated for causal inference over time. The procedure follows the same steps used in the SCM framework.

- **Abduction** Based on the observed trajectory  $\mathbf{X}_t$ , we estimate the values of  $\mathbf{u}_t$  by calculating the residuals  $\hat{\mathbf{u}}_t = \mathbf{X}_t - \mathbb{E}[\mathbf{X}_t | \mathbf{X}_{<t}]$ . For a VAR(p) model, in particular,  $\mathbb{E}[\mathbf{X}_t | \mathbf{X}_{<t}] = \mathbf{A}_1 \mathbf{X}_{t-1} + \dots + \mathbf{A}_p \mathbf{X}_{t-p}$ .
- **Action** We apply a specific intervention  $\mathcal{I}$  by modifying the model's equations.
- **Prediction** We simulate the evolution of the new process  $\mathbf{X}_t^{\mathcal{I}}$  using  $\hat{\mathbf{u}}_t$  in the equation.

Let  $\mathbf{X}_t$  be a time series generated by a VAR(p) model. We want to evaluate what the trajectory of  $\mathbf{X}_t$  would have been up to the present time  $t_1$  assuming a specific intervention was applied at a particular past time  $t_0$ . We proceed as follows:

1. Perform the abduction step and retrieve the residuals  $\{\hat{\mathbf{u}}_t\}_{t=t_0}^{t_1}$ .
2. Apply the intervention to the model as in App. C.2.
3. Simulate the counterfactual trajectory from  $\mathbf{X}_{t_0}$  to  $\mathbf{X}_{t_1}$  through the recursive application of

$$\mathbf{X}_t = \hat{\boldsymbol{\nu}} + \mathbf{A}_1 \mathbf{X}_{t-1} + \dots + \mathbf{A}_p \mathbf{X}_{t-p} + \hat{\mathbf{u}}_t.$$

where  $\hat{\boldsymbol{\nu}}$  is defined as in Eq. 25 or Eq. 26, depending on the type of intervention. Note that *if using forcing intervention*, the whole term on the right must be left-multiplied by  $[I + \mathbf{F}_{diag}]^{-1}$  before performing the simulation.

**Observation** Performing retrospective counterfactual without applying any intervention results in the perfect recovery of the factual trajectory, so that the difference with the interventional one can be interpreted in the same way as in C.2, i.e. as the causal effect over time along the trajectory.

## D Experimental details and extra results

In this section, we expand the description of the experimental section from §5, and provide the reader with additional results in the following subsections. First, we outline the details that are consistent across all experiments and then explore the specifics of each experiment in their respective subsections.

**Hardware** To run all experiments, we used a machine with 18 cores, 36 threads, equipped with Intel(R) Core (TM) i9-10980XE CPU @ 3.00GHz, OS Ubuntu 20.04.3, programming language Python 3.12.0.

**Datasets** This section provides all the information on datasets used in the empirical evaluation of §5 of the main manuscript and the following subsections.

**German** We aimed to capture relationships between the variables that appeared intuitive to us and, to a certain extent, reflected a real-world loan approval scenario. Therefore, we selected the following variables from the German Credit dataset<sup>11</sup>: *Expertise (E), Responsibility (R), Loan Amount (L), Loan Duration (D), Income (I), Savings (S) and Credit Score (C)*. We have indexed the variables from 0 to 6, following the sequence in which they are mentioned. The corresponding causal graph is designed as in Fig. 2b. To generate a 7-dimensional vector-valued stationary time series, we simulate a stable SVAR(4) process, considering four lags to be a reasonable timeframe for conducting our analysis. In modeling the autoregressive behavior of socio-economic variables, we use different matrices tailored to capture temporal dependencies in the data. Below, we provide interpretations for such matrices and specify all the non-zero coefficients:

- $A_0$  denotes the instantaneous impact between variables and affects only those nominal features (theoretical value of a good or financial instrument defined by a consensus or standard), e.g., the *Credit Score*. This is highlighted because the tangible attributes of an applicant require a

<sup>11</sup><https://www.kaggle.com/datasets/uciml/german-credit>

certain period to change. In our model, we set  $A_0[3, 6] = 0.5$ ;  $A_0[4, 6] = -0.3$ ;  $A_0[5, 6] = -0.5$ . Furthermore, all diagonal entries of  $A_0$  are set to 1;

- $A_1$  has diagonal values that are all 0.95 except for the last one (i.e., *Credit Score*), which is 0. This matrix gives the dynamic system a memory function.
- $A_2$  includes interactions among variables we classify as rapid. These effects are considered short-term and are typically the most direct and intense, as the system’s memory extends only one step back in time. In our model, we set  $A_2[1, 4] = 0.3$ ;  $A_2[2, 6] = 0.5$ ;  $A_2[4, 5] = 0.2$ ;
- $A_3$  contains medium-term effects, illustrating how conditions from three steps back affect the current state of the system. In our model, we set  $A_3[2, 3] = 0.5$ ;
- $A_4$  reflects long-term relationships within the system. In our model, we set  $A_4[0, 1] = 0.3$ ;  $A_4[0, 4] = 0.8$ .

**Pendulum** For the description of the model see App. B.3. To generate a 2-dimensional vector-valued stationary time series, we simulate a stable SVAR(1) process. In this case, we set  $A_0$  as an identity matrix, while  $A_1$  is set as in Eq. 23.

**Census** We consider open data extracted from the United States Census Bureau<sup>12</sup>. This source provides a panel dataset spanning yearly demographic characteristics for 227 countries, starting from 1950 up to 2023. We conducted a pre-processing procedure to align the data with our experimental requisites. Specifically, we selected the 50 countries with high income<sup>13</sup>. Since most countries had missing values in the initial decades of data collection, we decided to start the dataset from 1991, considering the 32-year period sufficient for our work. The total number of instances is therefore 1600. Then, we chose only the essential variables for our analysis, which led to the construction of the ground truth causal graph. The chosen variables include: *Total Population* for three age groups namely 0 – 14, 15 – 64, and 65 – 99, *Net Migration*, *Total Births*, *Total Deaths*. The assumed causal graph is shown in Fig. 2c. To adapt the data to the autoregressive model, we modified the assignment of values for *Net Migration*, *Total Births*, and *Total Deaths* by shifting them to the previous year’s values.

**Metrics** We measure the discrepancy between the  $h$ -step forecast  $\hat{X}_{t+h} | X_{<t}$  and the true value  $X_{t+h}$  on the test set using as metrics Root Mean Square Error (RMSE) and Symmetric Mean Absolute Percentage Error (SMAPE) (Montgomery, Jennings, and Kulahci 2015). We report scores focusing on the target variables (i.e., *Credit Score* for German,  $X^{(1)}$  for Pendulum, and age groups for Census).

**Training and evaluation methodology** We generated synthetic time-series datasets with varying training samples. We used 300 validation and 2400 test samples for German while 100 validation and 2200 test samples for Pendulum.

We implemented DLinear, TiDe, and TSMixer models using the Darts library (Herzen et al. 2022). Each model was

<sup>12</sup><https://www.census.gov>

<sup>13</sup><https://blogs.worldbank.org/en/odata/world-bank-country-classifications-by-income-level-for-2024-2025>

Table 3: **Observational forecasting.** MAE scores in Table 1. Here, we also report the standard deviation in subscript.

Dataset	Size	Horizon	MAE				
			Oracle	VAR	DLinear	TiDE	TSMixer
German	100	1	.004	<b>.008</b> <sub>.004</sub>	.009 <sub>.004</sub>	.011 <sub>.000</sub>	.014 <sub>.001</sub>
Pendulum			.042	<b>.043</b> <sub>.001</sub>	<b>.043</b> <sub>.001</sub>	.218 <sub>.000</sub>	.217 <sub>.000</sub>
German	100	10	.014	<b>.055</b> <sub>.030</sub>	<b>.055</b> <sub>.027</sub>	.094 <sub>.003</sub>	.139 <sub>.005</sub>
Pendulum			.399	<b>.420</b> <sub>.018</sub>	.440 <sub>.009</sub>	1.43 <sub>.002</sub>	1.43 <sub>.001</sub>
German	500	1	.004	<b>.004</b> <sub>.000</sub>	<b>.004</b> <sub>.000</sub>	.011 <sub>.000</sub>	.014 <sub>.000</sub>
Pendulum			.042	<b>.042</b> <sub>.000</sub>	<b>.042</b> <sub>.000</sub>	.218 <sub>.001</sub>	.217 <sub>.000</sub>
German	500	10	.014	<b>.015</b> <sub>.001</sub>	<b>.015</b> <sub>.000</sub>	.093 <sub>.002</sub>	.135 <sub>.004</sub>
Pendulum			.399	<b>.401</b> <sub>.002</sub>	.405 <sub>.010</sub>	1.43 <sub>.003</sub>	1.43 <sub>.001</sub>

trained for 200 epochs, with final evaluations performed on the test set. We employed an early stopping mechanism to prevent overfitting, monitoring the validation loss with patience set to 10 and a minimum delta of  $1e - 5$ . We used the Adam optimizer (Kingma and Ba 2015) with an initial learning rate of  $1e - 3$  and an exponential learning rate scheduler<sup>14</sup> with a decay rate of 0.99. For hyperparameter tuning, we always select the best hyperparameter combination according to validation loss, reporting results from the test dataset in the manuscript. We applied Mean Squared Error as the loss function for DLinear and quantile regression as the likelihood function for TiDE and TSMixer.

For the Census dataset, we constrained the fitting of the VAR framework by setting the matrix coefficients without dependencies in the causal graph to zero.

All experiments were repeated 10 times, with results reported as averages and standard deviations.

## D.1 Observational Forecasting

**How does the VAR performance compare with SOTA models for forecasting multivariate time series?** Table 3 presents results that mirror those in Table 1 with standard deviation in subscript. In addition to the results from §5.1, Table 4 provides the forecasting accuracy, measured using RMSE and SMAPE scores, across different data sizes and forecast horizons for German and Pendulum datasets. The patterns observed here are consistent with those in the main text. VAR continues to lead in performance, often aligning closely with the Oracle. DLinear remains competitive for shorter forecast horizons thanks to its linear structure, occasionally surpassing VAR by a small margin.

In contrast, TSMixer and TiDE generally underperform in comparison, with their scores consistently following behind VAR and DLinear. The challenging nature of the Pendulum dataset is apparent, with all models (including Oracle) showing greater difficulty in maintaining the accuracy as for German. Table 5 presents the results for the Census dataset. The performance gap between the models narrows. For 1-step

<sup>14</sup>[https://pytorch.org/docs/stable/generated/torch.optim.lr\\_scheduler.ExponentialLR.html](https://pytorch.org/docs/stable/generated/torch.optim.lr_scheduler.ExponentialLR.html)

Table 4: **Observational forecasting.** RMSE and SMAPE scores (*lower is better*) for VAR, DLinear (Zeng et al. 2023), TiDE (Das et al. 2023) and TSMixer (Chen et al. 2023), benchmarked against the oracle forecaster. Results averaged over ten runs, with standard deviation in subscript.

Dataset	Size	Horizon	RMSE					SMAPE				
			Oracle	VAR	DLinear	TiDE	TSMixer	Oracle	VAR	DLinear	TiDE	TSMixer
German Pendulum	100	1	.005	<b>.010</b> <sub>.004</sub>	.011 <sub>.005</sub>	.063 <sub>.009</sub>	.071 <sub>.002</sub>	2.01	<b>3.81</b> <sub>1.44</sub>	4.12 <sub>1.56</sub>	14.6 <sub>2.16</sub>	20.4 <sub>0.33</sub>
			.053	<b>.053</b> <sub>.001</sub>	.054 <sub>.001</sub>	.333 <sub>.033</sub>	.264 <sub>.000</sub>	15.7	<b>15.8</b> <sub>0.22</sub>	15.8 <sub>0.23</sub>	62.0 <sub>3.73</sub>	54.2 <sub>0.00</sub>
German Pendulum	100	10	.018	.069 <sub>.038</sub>	<b>.068</b> <sub>.033</sub>	.306 <sub>.053</sub>	.284 <sub>.008</sub>	7.33	17.2 <sub>6.14</sub>	<b>17.0</b> <sub>5.36</sub>	53.7 <sub>3.75</sub>	58.8 <sub>0.46</sub>
			.494	<b>.520</b> <sub>.022</sub>	.545 <sub>.013</sub>	1.89 <sub>.069</sub>	1.74 <sub>.000</sub>	82.7	<b>87.2</b> <sub>4.61</sub>	88.9 <sub>3.21</sub>	175 <sub>2.32</sub>	180 <sub>0.03</sub>
German Pendulum	500	1	.005	<b>.005</b> <sub>.000</sub>	<b>.005</b> <sub>.000</sub>	.037 <sub>.003</sub>	.074 <sub>.002</sub>	2.01	2.15 <sub>0.08</sub>	<b>2.13</b> <sub>0.08</sub>	8.45 <sub>0.46</sub>	17.7 <sub>0.44</sub>
			.053	<b>.053</b> <sub>.000</sub>	<b>.053</b> <sub>.000</sub>	.352 <sub>.014</sub>	.264 <sub>.000</sub>	15.7	<b>15.7</b> <sub>0.02</sub>	<b>15.7</b> <sub>0.03</sub>	63.8 <sub>1.72</sub>	54.2 <sub>0.00</sub>
German Pendulum	500	10	.018	<b>.019</b> <sub>.001</sub>	<b>.019</b> <sub>.001</sub>	.200 <sub>.014</sub>	.320 <sub>.008</sub>	7.33	<b>7.55</b> <sub>0.19</sub>	7.68 <sub>0.20</sub>	40.9 <sub>1.63</sub>	56.5 <sub>0.35</sub>
			.494	<b>.496</b> <sub>.002</sub>	.502 <sub>.011</sub>	1.93 <sub>.030</sub>	1.74 <sub>.000</sub>	82.7	<b>83.3</b> <sub>0.75</sub>	83.8 <sub>1.08</sub>	174 <sub>0.70</sub>	180 <sub>0.04</sub>
German Pendulum	1000	1	.005	<b>.005</b> <sub>.000</sub>	<b>.005</b> <sub>.000</sub>	.025 <sub>.001</sub>	.051 <sub>.002</sub>	2.01	2.09 <sub>0.03</sub>	<b>2.07</b> <sub>0.04</sub>	6.57 <sub>0.21</sub>	12.4 <sub>0.41</sub>
			.053	<b>.053</b> <sub>.000</sub>	<b>.053</b> <sub>.000</sub>	.373 <sub>.018</sub>	.264 <sub>.000</sub>	15.7	<b>15.7</b> <sub>0.02</sub>	<b>15.7</b> <sub>0.03</sub>	65.9 <sub>1.89</sub>	54.1 <sub>0.01</sub>
German Pendulum	1000	10	.018	<b>.018</b> <sub>.000</sub>	<b>.018</b> <sub>.000</sub>	.161 <sub>.006</sub>	.264 <sub>.007</sub>	7.33	<b>7.38</b> <sub>0.09</sub>	7.43 <sub>0.13</sub>	34.2 <sub>0.66</sub>	51.8 <sub>0.84</sub>
			.494	<b>.495</b> <sub>.001</sub>	.498 <sub>.006</sub>	1.97 <sub>.037</sub>	1.74 <sub>.000</sub>	82.7	<b>82.8</b> <sub>0.54</sub>	83.2 <sub>0.66</sub>	173 <sub>0.90</sub>	180 <sub>0.01</sub>

Table 5: **Observational forecasting.** RMSE and SMAPE scores (*lower is better*) for VAR, DLinear, TiDE and TSMixer on the Census dataset.

Dataset	Size	Horizon	RMSE				SMAPE			
			VAR	DLinear	TiDE	TSMixer	VAR	DLinear	TiDE	TSMixer
Census	50×32	1	<b>.002</b>	.007	<b>.002</b>	.009	.409	1.76	<b>.401</b>	1.79
		5	.018	.026	<b>.013</b>	.024	3.25	6.36	<b>2.92</b>	6.28

forecasts, both VAR and TiDE achieve similar, strong results, while for 5-step forecasts, TiDE slightly outperforms VAR in both metrics.

## D.2 Interventional Forecasting

**How do additive and forcing interventions affect the system dynamics?** Fig. 9 illustrates two additive interventions applied to German. Panel (a) depicts an intervention on *Responsibility* with  $F = -0.3$ , while panel (e) shows an intervention on *Loan Amount* with  $F = 0.5$ . The causal graphs in panels (d) and (h) show how these interventions propagate through the network. Panels (b) and (c) display the effects of the *Responsibility* intervention on *Loan Duration* and *Income*, respectively. Panels (f) and (g) illustrate the corresponding effects for the *Loan Amount* intervention. Specifically, in panels (a-c), we observe that the intervention on *Responsibility* affects *Income* while having no impact on *Loan Duration*. This behavior aligns with the causal relationships depicted in panel (d) as *Responsibility* is not an ancestor of *Loan Duration*. Similarly, panels (e-g) illustrate that the intervention on *Loan Amount* affects only *Loan Duration*, as *Loan Amount* is not an ancestor of *Income*.

Fig. 10 shows two forcing interventions applied to German. Panel (a) displays an intervention on *Income* with

$F = 5$  and target value  $\hat{I} = 20$ . Panels (b) and (c) show how this intervention affects *Savings* and *Credit Score*, respectively. Panel (e) presents an intervention on *Loan Duration* with  $F = 3$  and target value  $\hat{D} = 4$ , while panel (f) shows a different intervention on *Income* with  $F = 3$  and target value  $\hat{I} = 20$ . Panels (a-c) present results that are consistent with those demonstrated in the manuscript, namely that interventional forecasting precisely aligns with the specified target value. Panels (e-f) demonstrate the capability of the causal VAR framework to implement multiple interventions within the system simultaneously. Panel (g) displays the combined impact of these interventions on *Credit Score*. By visualizing this cumulative effect, we could gain insights into the complex interplay between multiple variables and their joint influence on the target variable.

**Interventions** We provide the intervention type and the force values used to evaluate the interventional forecasting described in the following paragraph. For German, we perform causal interventions on root node *Expertise*, and observe the resulting effect on the target variable *Credit Score*. For the additive case, we apply  $F = 0.2$ , while for the forcing case, we use  $F = 1$  with a target value of  $\hat{E} = 5$ . For Pendulum, we perform causal interventions on  $X^{(2)}$ , and ob-

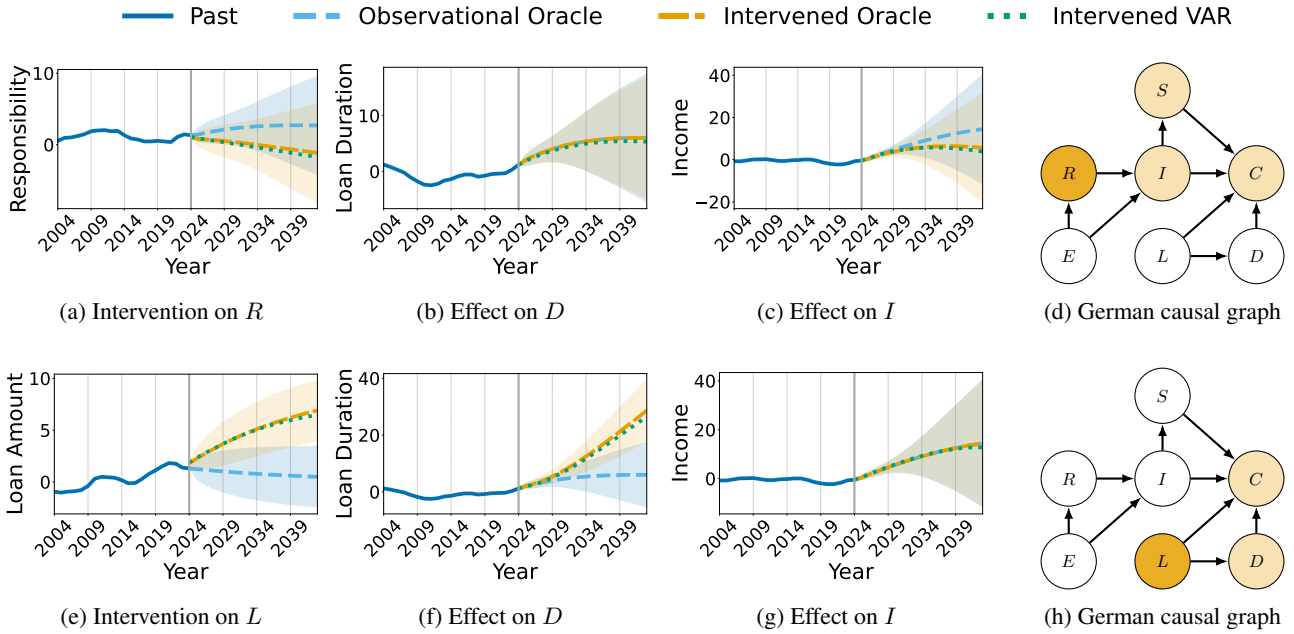


Figure 9: **Additive Interventions.** (a) Intervention on *Responsibility* with  $F = -0.3$  and the resulting effect on: (b) *Loan Duration* and (c) *Income*. (e) Intervention on *Loan Amount* with  $F = 0.5$  and the resulting effect on: (f) *Loan Duration* and (g) *Income*. In (d) and (h), the deep orange node represents the intervened variable, while the lighter orange nodes are those influenced by the intervention. In all plots, shaded regions denote 95% confidence bounds.

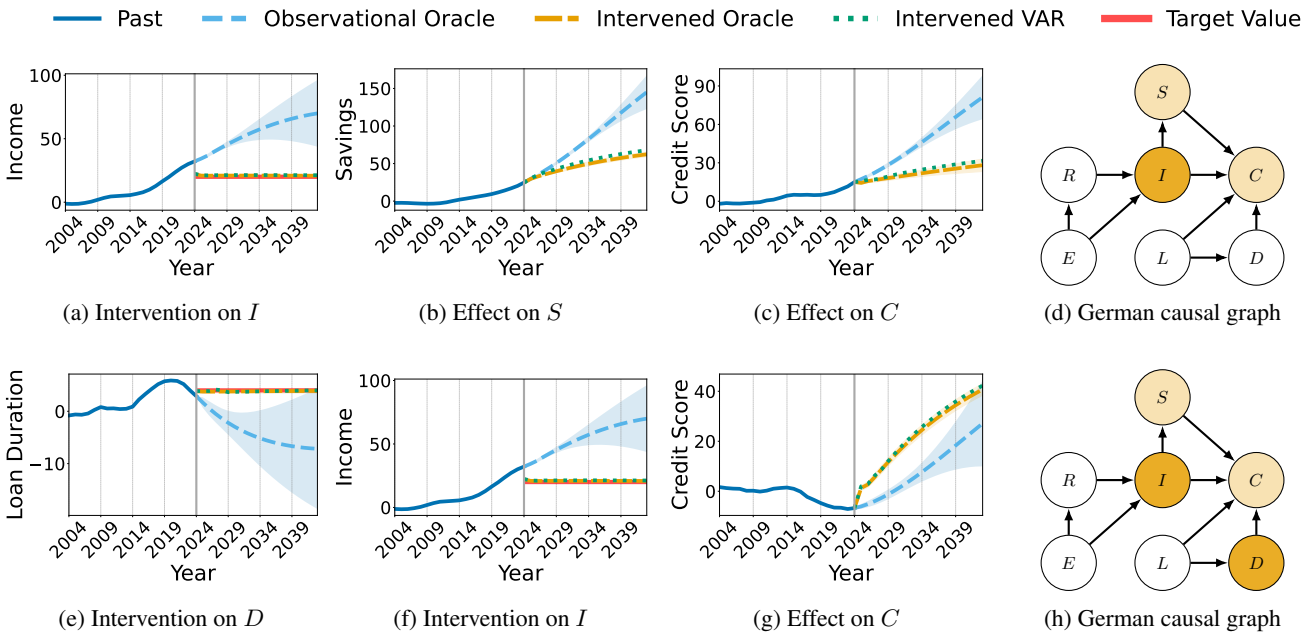


Figure 10: **Forcing Interventions.** (a) Intervention on *Income* with  $F = 5$  and target value  $\hat{I} = 20$ . The resulting effect on (b) *Savings* and (c) *Credit Score*. (e) Intervention on *Loan Duration* with  $F = 3$  and target value  $\hat{D} = 4$ . (f) Intervention on *Income* with  $F = 3$  and target value  $\hat{I} = 20$ . (g) Effect of interventions in (e-f) on *Credit Score*. In (d) and (h), the deep orange node represents the intervened variable, while the lighter orange nodes are those influenced by the intervention. In all plots, shaded regions denote 95% confidence bounds.

Table 6: **Interventional Forecasting.** RMSE and SMAPE scores (*lower is better*) for the proposed causal VAR framework on German and Inverted Pendulum datasets. RMSE scores are scaled by a factor of  $10^2$  to ease readability. Results averaged over ten runs, with standard deviation in subscript.

Dataset	Train Steps	Horizon	RMSE (scaled)		SMAPE	
			Additive	Forcing	Additive	Forcing
German Pendulum	100	1	.000.000 .042.031	.000.000 .062.046	.000.000 .146.107	.000.000 .319.236
		10	.446.295 6.664.47	1.531.27 .102.051	.829.547 2.191.57	5.804.57 .262.140
German Pendulum	500	1	.000.000 .024.023	.000.000 .035.034	.000.000 .083.080	.000.000 .180.173
		10	.173.139 2.021.52	.464.338 .049.035	.353.276 .690.451	1.891.33 .111.077
German Pendulum	1000	1	.000.000 .010.007	.000.000 .014.011	.000.000 .034.026	.000.000 .074.056
		10	.101.079 1.11.853	.299.220 .023.012	.210.163 .376.257	1.24.892 .054.031

Table 7: **Interventional Forecasting.** MAE scores (*lower is better*) for the proposed causal VAR on the Pendulum dataset. Results averaged over 10 runs, with standard deviation in subscript. Scores are scaled by a factor of  $10^3$  to ease readability.

Dataset	Train Steps	Horizon	MAE	
			Additive	Forcing
Pendulum	100	1	.094.069	.310.230
		10	6.324.44	.264.142
	500	1	.053.052	.174.169
		10	1.951.39	.112.078

serve the resulting effect on  $X^{(1)}$ . For the additive case, we apply  $F = 0.4$ , while for the forcing case, we use  $F = 1$  with a target value of  $\hat{X}^{(2)} = 1$ .

**How accurate is the causal VAR framework in estimating the causal effect of interventions over time?** Table 6 provides RMSE and SMAPE scores for interventional forecasting across different data sizes and forecast horizons on the German and Pendulum datasets. These scores further validate the effectiveness of the proposed causal VAR framework. For 1-step forecasts, the Pendulum dataset shows the intervention effect immediately, in contrast to the German dataset, where variables change slowly and require several time steps to exhibit measurable effects. For 10-step forecasts, the scores demonstrate that the model achieves high accuracy. Notably, the RMSE values remain low across both datasets and intervention types, indicating the robustness of the model in estimating causal effects over longer horizons.

Additionally, while the SMAPE scores show some variation, the results suggest that the model is well-suited for handling more complex forecasting scenarios.

Table 7 outlines the results of interventional forecasting, detailing errors across different data sizes and forecast horizons for the Pendulum dataset. Our causal effect estimates remain highly accurate for both forecast horizons. In contrast to the German dataset in Table 2, the intervention effect is observable even at the 1-step forecast. These results reinforce the findings presented in the main paper, highlighting the effectiveness of the proposed causal VAR framework in interventional forecasting tasks.

### D.3 Retrospective Counterfactuals

In this section, we demonstrate that our causal VAR framework can also address the causal queries discussed §4.3 in terms of retrospective counterfactuals.

Fig. 11 illustrates two counterfactual interventions, with panels (a-d) related to German and panels (e-h) focused on Census. For German, panel (a) shows an intervention in 2004 on *Expertise* with  $F = 0.3$  and the effect of this intervention on (b) *Responsibility* and (c) *Loan Amount*. This scenario could potentially answer the question: “What would be the outcome in 2024 if an applicant had improved their expertise in 2004?”. Panel (b) shows that an increase in *Expertise* would have led to a corresponding rise in *Responsibility*. Notably, panel (c) reveals the *Loan Amount* remains unchanged, reflecting the structure of our causal graph where *Expertise* is not an ancestor of this node. For the Census dataset, we examine an intervention in 2011 on *Births* with  $F = 0.004$  and its effect on the population’s average age (computed as a weighted mean of age groups) of three countries: (e) Germany, (f) Spain, and (g) Singapore. The force value indicates that *Births* increase by 0.4% of each coun-

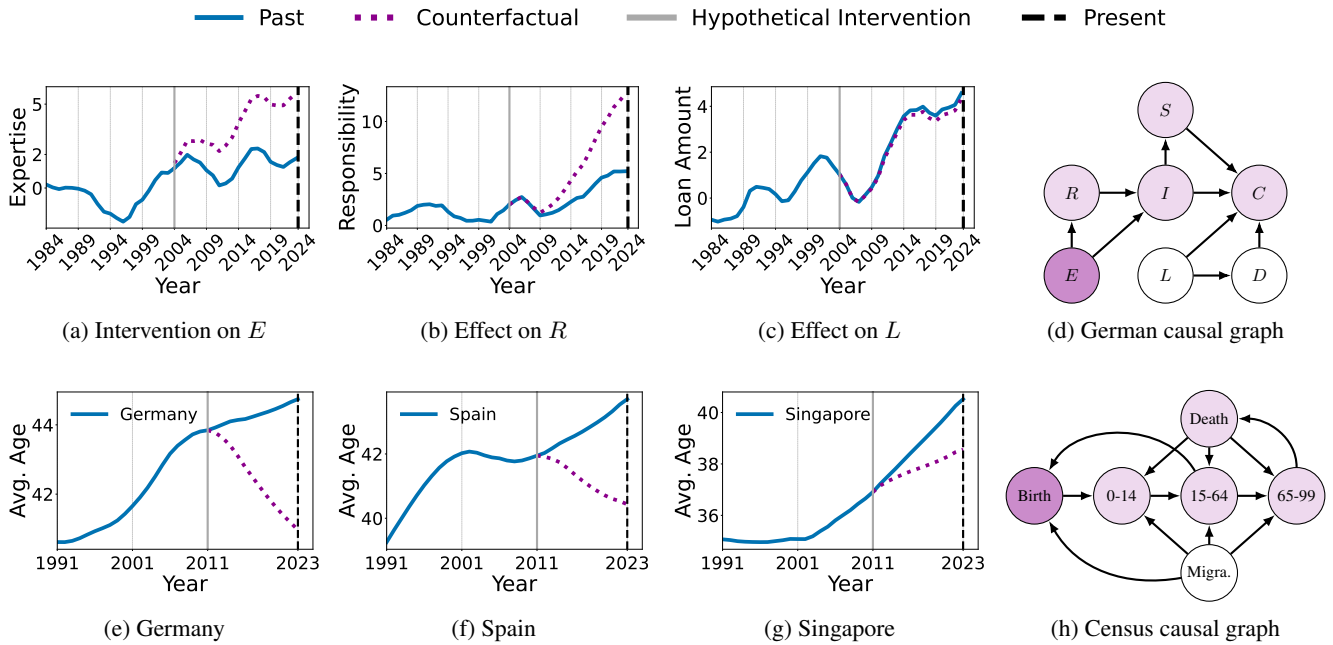


Figure 11: **Retrospective Counterfactuals**. Panels (a-d) focus on the German dataset. (a) Intervention on *Expertise* with  $F = 0.3$ . Effect of the intervention on (b) *Responsibility* and (c) *Loan Amount*. Panels (e-h) examine the Census dataset with an intervention on *Births* with  $F = 0.004$ . Effect of the intervention on the population's average age of (e) Germany, (f) Spain, and (g) Singapore. In (d) and (h), the deep purple node represents the intervened variable, while the lighter purple nodes are those influenced by the intervention.

try's total population annually. This analysis could potentially explore the question: "How would a policy promoting increased births in 2011 have affected a country's current average population age?". Panels (e-f) display that such an intervention would have significantly lowered the average age in Germany and Spain, given their relatively older population structures. In contrast, panel (g) shows that the effect on Singapore would have been more moderate, consistent with its younger demographic profile at the intervention time.